



Nordic Community for Fast Steel Heat Treatments (NorFaST-HT)



Interreg Nord 2014-2020: Research and innovation
3 years (+SWERIM extension) project (5/2015–10/2018)
~1.7 M€ budget
antti.jarvenpaa@oulu.fi (+358445551633)

Introduction

The NorFaST-HT -project was executed to establish the “Nordic Community for Fast Steel Heat Treatments”, having resources and expertise for design and simulation of customer-based heat treatments. The project consortium included universities at Oulu, Luleå and Lund, in addition to a research organisation SWERIM in Luleå. The industrial partners were SSAB, Outokumpu, Miilux, Swebor Stål, Olofsfors and MagComp. The project included different research activities such as induction technology development, establishing new laboratories and material development. This report describes the main achievements and future chances **which** have been realized during the project.

Content of the report

This report has been divided into three chapters as listed below:

- Chapter 1: Laboratory facilities for academic and industrial heat treatment experiments
- Chapter 2: Material technical applications for fast steel heat treatments
- Chapter 3: Future induction heating and material research

Chapter 1 - Laboratory facilities for academic and industrial heat treatment experiments

NorFaST-HT research facilities are located in several locations. The University of Oulu has its induction and laser heating laboratory in Nivala, Finland (ELME-studio) and a laser heating laboratory is in Luleå at Luleå University of Technology. During the project, new induction heating laboratories were founded at the Lund University and MEFOS. All the laboratories have a certain kind of specialization to complete each other. The laboratories are described in the following sections (Sections 1.1–1.3).

- 1.1 Heat treatment laboratory at the Nivala ELME-studio
- 1.2 Induction heating facilities at Lund University
- 1.3 Induction heating facility at SWERIM (Luleå)
- 1.4 Laser processing laboratory at LTU (Luleå)



1.1 Heat treatment laboratory at the Nivala ELME-studio

A prototype induction furnace (MP600, Figs. 1–5) capable for research purposes (wide range of sample geometries) was designed and manufactured at French Fives Celes Company during the year 2013 (installed at Nivala in November 2013). The heater is fixed together with a roller line and a quenching unit, as shown in Fig. 2. The axial (copper tube) MP600 inductor has a limited efficiency above the Curie point of ferritic metals and over the whole temperature range of FCC metals. The limitation is realized as a low line speed in the austenitization processes (e.g. hardening, Section 2.1.2). The active coil is only 200 mm long (green lines in Fig. 4) to maximize the heating rate. Heat is formed at approximately 1.6 mm deep layers (skin-effect) in the workpiece, but the temperature is relatively uniform along the thickness during continuous annealing in the thickness range of 3.5–6.5 mm. Feeding of metal sheets was carried out using roller table modules (1600 x 1700 mm, L x W), a chain drive, an electrical motor (1.5 kW) with a frequency converter (ABB ACS880 Series) and a dummy-plate for bonding the test plates precisely with the alignment of the roller line. In addition to the MP600 unit, a 25 kW power source (MP25) was purchased for various types of coils (Fig. 6–9). The MP25 power source operates at the frequency range between 100 and 400 kHz and it can also be used for surface processing of metals.

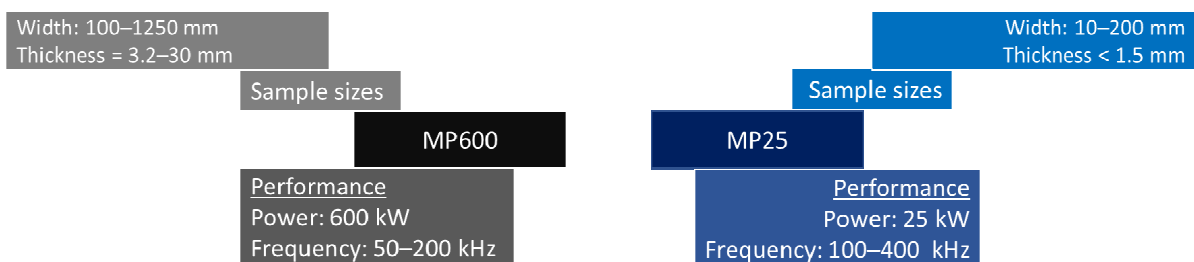


Fig. 1. Induction heating units at Nivala. Both units (MP600 and MP25) can be used in the continuous mode, so that the sample length is flexible.

The following updates were executed for the main induction line during the project:

- Quenching system
 - New protective covers were designed, manufactured and installed to prevent water leakage to the hall space (Fig. 3a)
 - A new air curtain was designed, manufactured and installed to prevent water leakage to the inductor (Fig. 3b)
 - Housing was reinforced to increase the quenching pressure from 1.5 to 10 bars
 - Pneumatic valves were installed to control the water circulation to improve the usability of the line
- Instrumentation and digital solutions
 - The pyrometer was relocated as shown in Fig. 4a. Earlier the pyrometer measured the temperature at approximately 20 cm distance from the coil. The measured value was always lower than the true maximum temperature due to self-cooling. In the newest solution, the pyrometer measures the temperature just after the coil to minimize the influence of self-cooling and is now more accurate (Figs 4b and 4c).
 - Instrumented (water levels, etc.) water circulation to increase the safety and usability of the line)
 - Instrumented (speed, etc.) roller line for increased safety features
 - Remote control for all the electrical devices (Fig. 5)
- Sheet support systems
 - A new support system was built for heating very thin sheets while using the MP25 unit (Fig. 6)
- Heating solutions



- A capacitor tank was purchased for the MP25 unit to add the possibility to utilize “random-shaped” coils for various applications
- Three new inductors (MP25 unit) were purchased, for example for pipe applications (Fig. 7)
- A robot was installed besides the induction line to move either workpieces or inductors (Fig. 7–9).

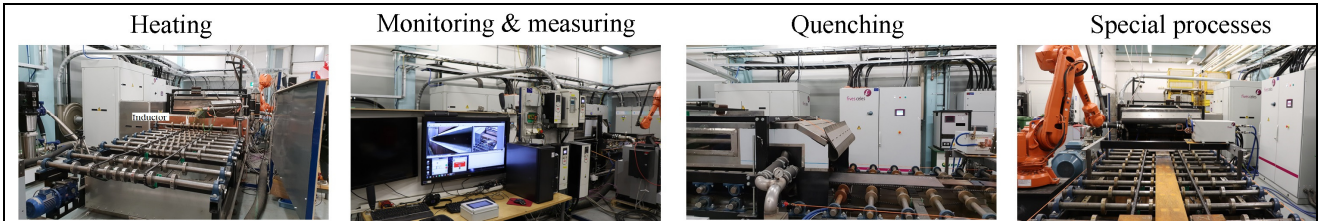


Fig. 2. The Nivala induction line.

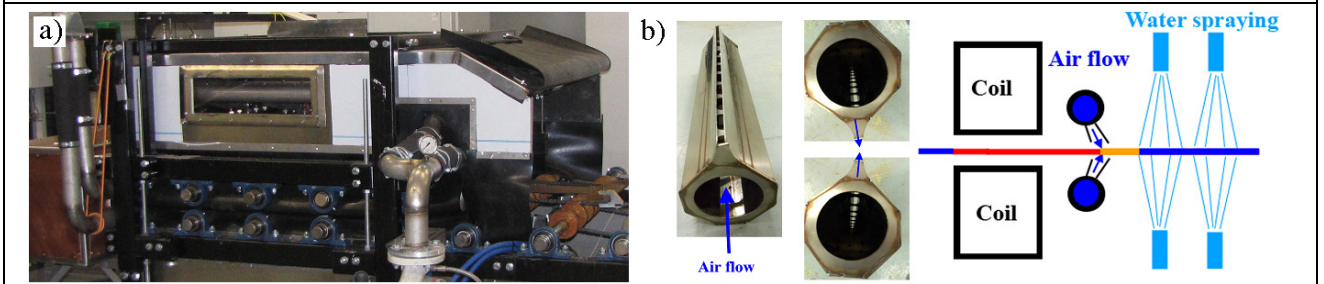


Fig. 3. Photos showing a) updated quenching unit and b) the newest air curtain system.

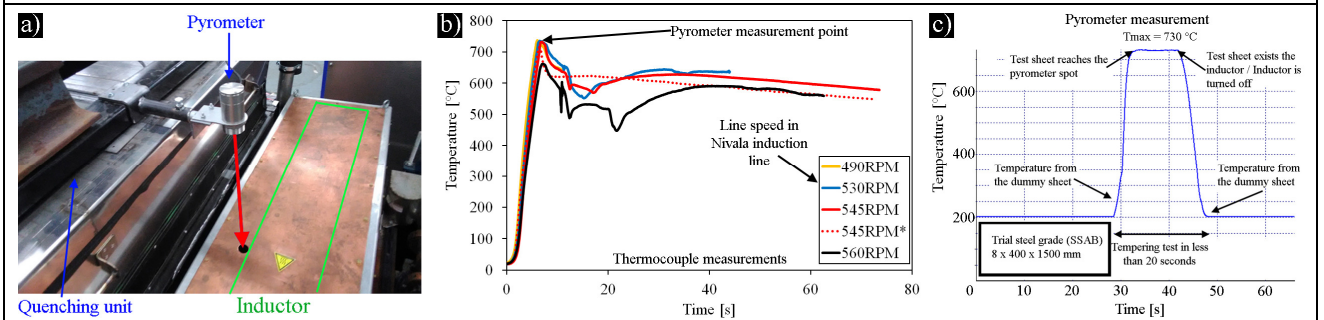


Fig. 4. a) New installation for the optical temperature measurements (Optris CT3MH2-SS pyrometer) to record reliably the peak temperature. b) and c) An example case from induction tempering of an 8 mm (400 x 1500 mm, W x L) thick steel piece. The middle figure shows the temperature history measured by thermocouples and the right one a pyrometer measurement curve.

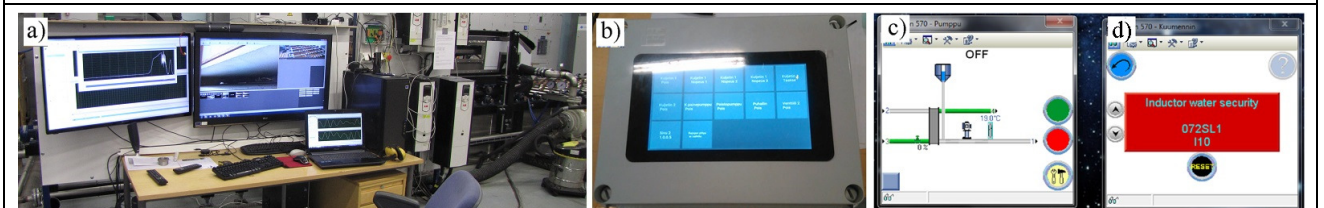


Fig. 5. a) New control systems for b) sheet feed and water circulation, c) inductor and d) cooling unit.



Fig. 6. Sheet support system for the MP25 “knife inductor”.

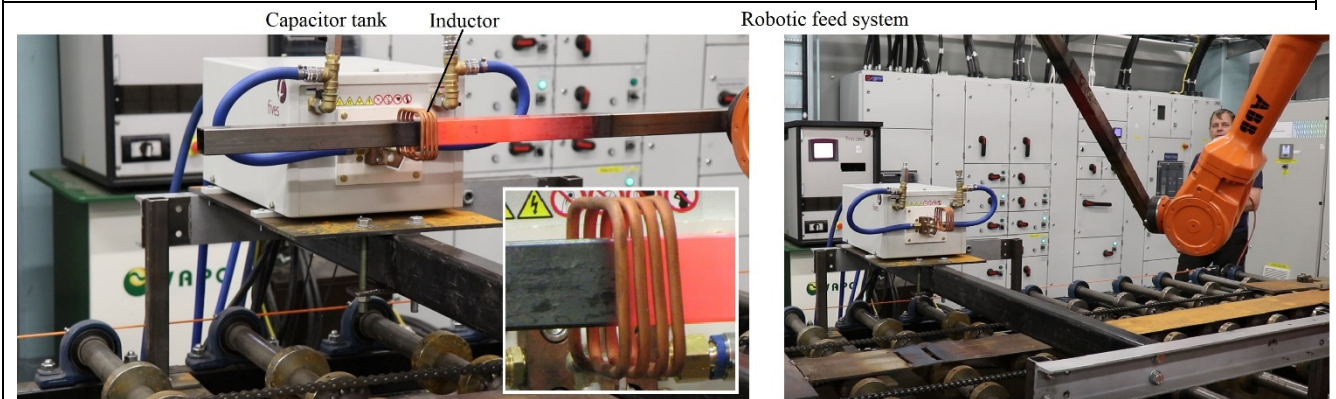


Fig. 7. The updated MP25 unit (capacitor tank + inductors) showing a coil for rectangular pipes as an example.

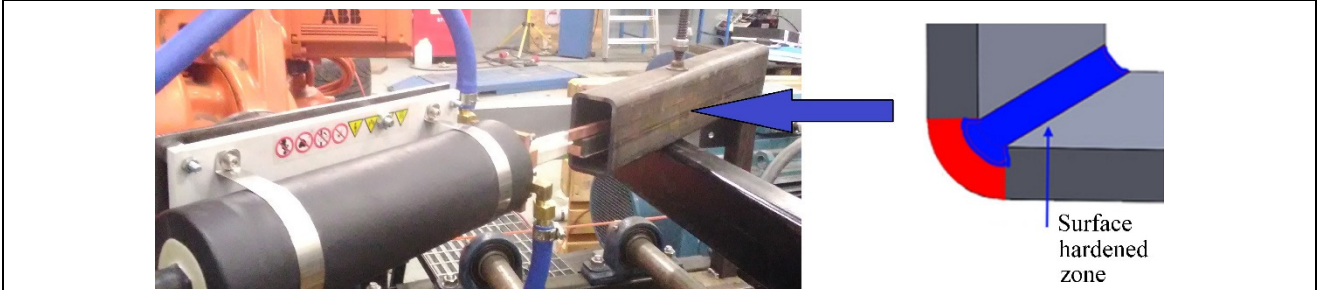


Fig. 8. The updated MP25 unit (capacitor tank + inductors) showing a coil for annealing inner corners (formed structures) as an example.

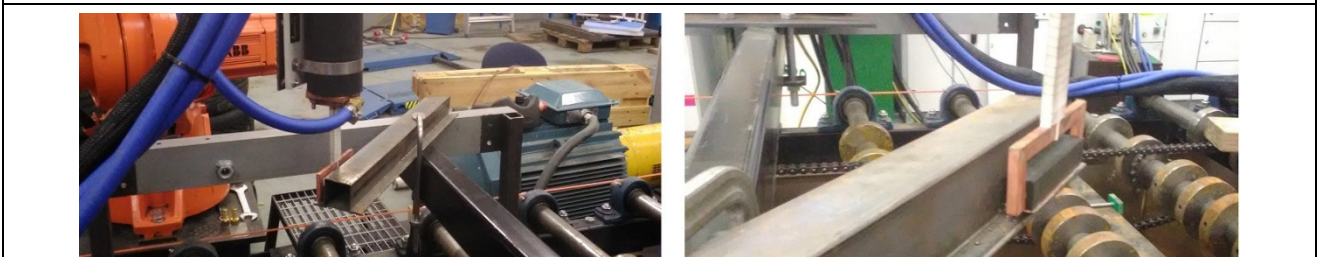


Fig. 9. The updated MP25 unit (capacitor tank + inductors) showing a coil for annealing outer corners (welded structures) as an example.



1.2 Induction heating facilities at Lund University

Lund University and its spin-off company MagComp Ab were focusing on the development of induction technology during the NorFaST-HT project. The selected research results are presented in Section 3.1, but in addition to the fundamental research, the Lund groups have designed and manufactured two different induction heating units for the community (Fig. 10). The both units are based on transversal flux inductors. The unit 1 (Fig. 11), “Laboratory unit”, is made for rapid hardening experiments and it only has a single transversal flux pair. The unit includes a sheet feed system to transfer the sheet first through the inductor to reach the desired maximum temperature and then to transfer the hot sheet rapidly to the water tank for immediate quenching. The unit 2 (Fig. 12), “Demonstrator unit”, is for demonstrating the effect of tilt angle of the coil pairs on heat distribution (edge overheating). The main limitation of the transversal flux technology is the edge temperature control. In practice, transversal heaters are fixed for a constant sheet width to prevent overheating on the edges. The NorFaST-HT solution is to adjust the angle of the inductors to prevent the edge overheating. In addition to demonstrate this feature, the demonstrator unit can also be used to simulate materials engineering phenomena with thin sheets (e.g. reversion treatment, Section 2.3).

Simulation models are important tools for analyzing the result in induction heating processes. To have a good correlation between a model and reality, accurate experimental data of the material properties must be used. To develop induction technology, the Lund group also has a system based on induction heating to measure physical material properties (Fig. 13). The method was utilized to determine these properties at a number of discrete temperatures, ranging from room temperature to 900 °C. A supplementary internal report.

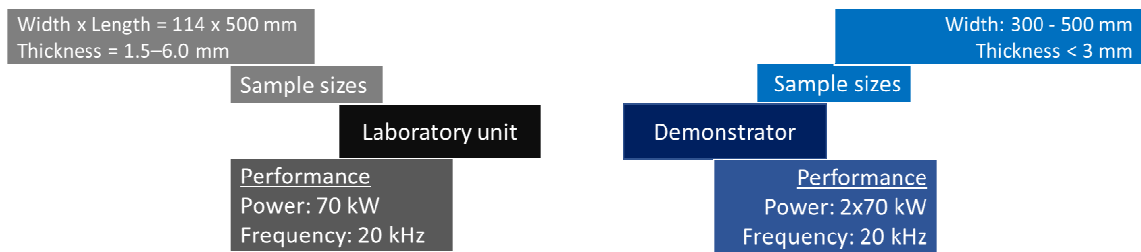


Fig. 10. Induction heating units in Lund.

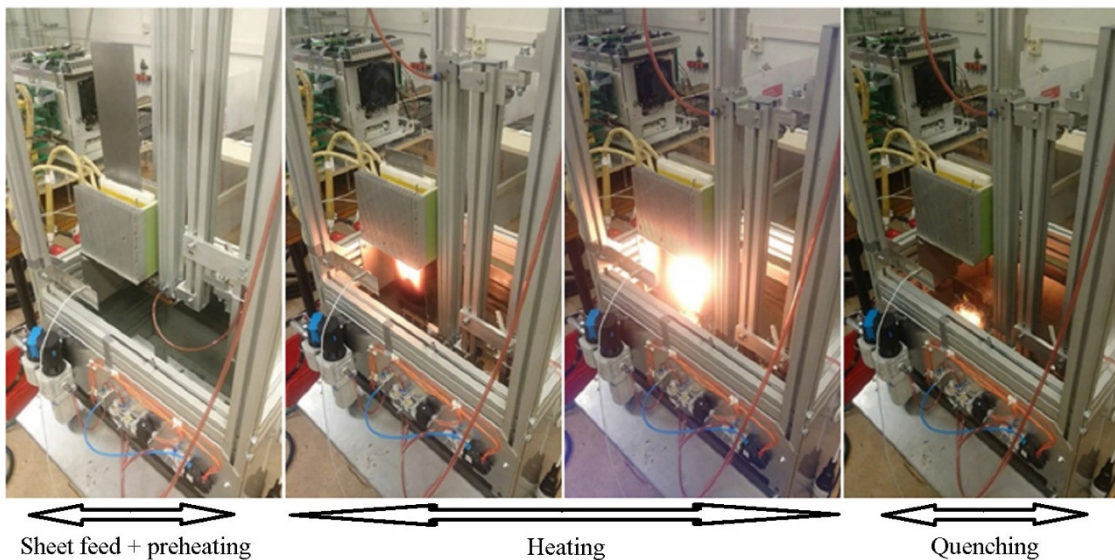


Fig. 11. “The laboratory unit” at the Lund University. Transverse inductor with sheet transfer system and quenching tank.

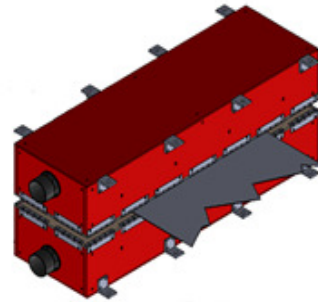
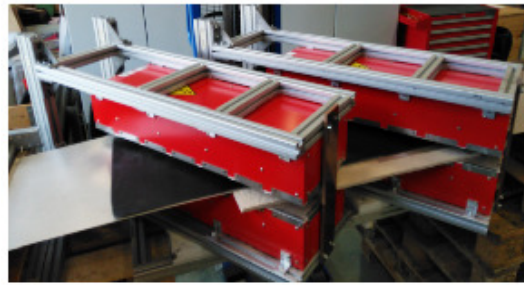


Fig. 12. “The demonstrator unit” at the Lund University / MagComp Ab.

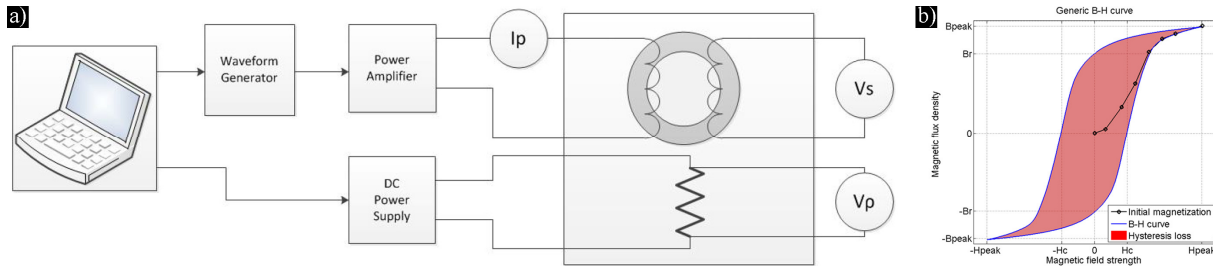


Fig. 13. a) Schematic illustration of the measurement setup. I_p is the excitation current, V_s is the induced voltage. 4-wire resistance measurement is supplied by a constant DC current and V_p is the sensed voltage drop. b) Generic B-H curve illustration with remanence, coercivity and hysteresis loss as well as the initial magnetization curve.

Publications, reports, presentations...

- “High Temperature Measurements of Electric and Magnetic Properties – Methodology”: Describes the methodology in detail (Lund)
- “Electric and Magnetic Data for B27, Boron steel, SSAB/Rautaruukki”: Physical properties for the boron steels (Lund)
- T. Cedell, K. Frogner, M. Andersson, QUADHEATER - UNIFORM HEATING WITH TRANSVERSAL INDUCTION COILS
- F. Lundström, K. Frogner, L. Siesing, V. Akujärvi, T. Cedell, M. Andersson, Cooling of Litz Wires in Industrial Induction Heating Applications
- V. Akujärvi, K. Frogner, T. Cedell, M. Andersson, Inductive temperature measurement for industrial induction heating applications

1.3 Induction heating facility at SWERIM (Luleå)

SWERIM had an existing continuous cold rolling mill in their facilities which was updated during the project with induction heaters and a quenching unit to be able to perform a continuous process from hot rolling to quenching using narrow coils. In the developed solution, the heating is carried out in two stages. Two types of inductors are implemented to increase the total efficiency in continuous austenization process. Both inductors have a power of 100 kW and the frequency is optimized for each temperature range (below or above the Curie-point). The line (Figs. 14–16) is designed for relatively narrow specimens (up to about 40 mm). The small width (volume) of the material and the high heating power (200 kW) with a high line speed enable to study fast steel heat treatments in a continuous process. The line was also equipped with a new custom-made and flexible quenching unit. New security features were designed and installed such as additional grounding of strip, mill and stands to meet the requirements for electrical safety. The heaters and quenching unit were equipped with protective transparent hoods, as well as warning lights and a machine emergency stop button were included to the control system.

The main advantages in comparison to the Nivala line are for instance: 1) hot rolling possibility, 2) high heating rate over the whole temperature range and 3) short delay between finishing the heating and start of the



quenching. The line can be applied to simulate the production at high-volume steel manufacturers. For example, the chance for the DQ&P (direct quenching and partitioning) experiments was added by optimizing the quenching unit (Figs. 17 and 18).

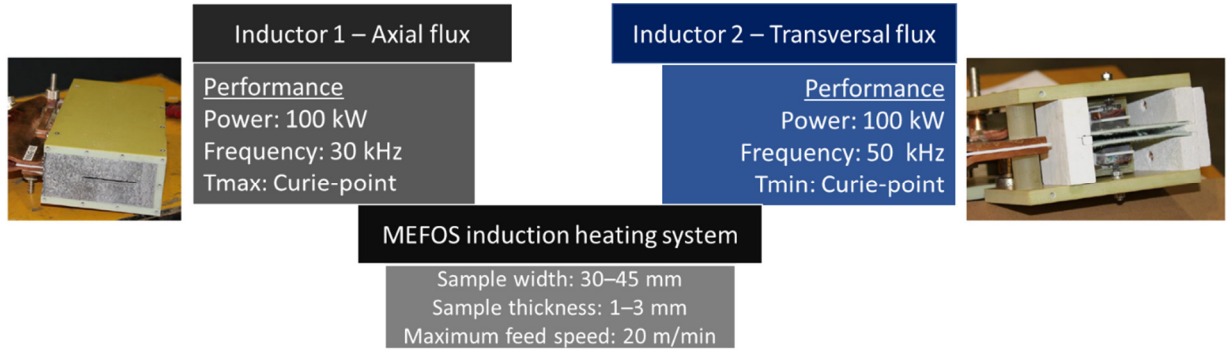


Fig. 14. Inductors in the MEFOS induction line.

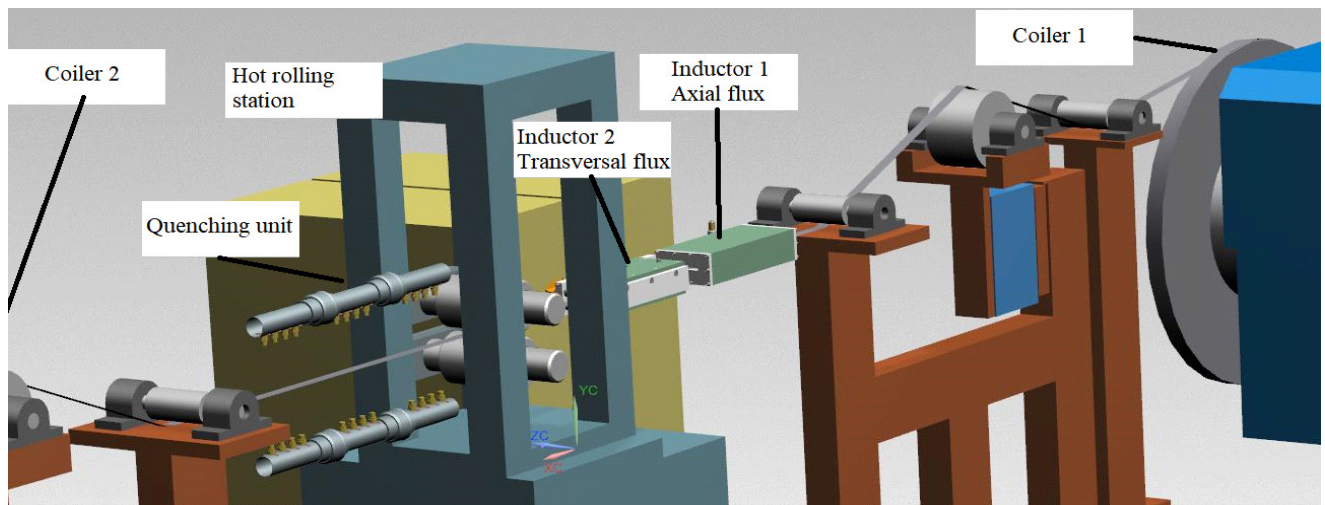


Fig. 15. Schematic illustration of the MEFOS induction line with a hot rolling stand, a quenching unit and coilers.

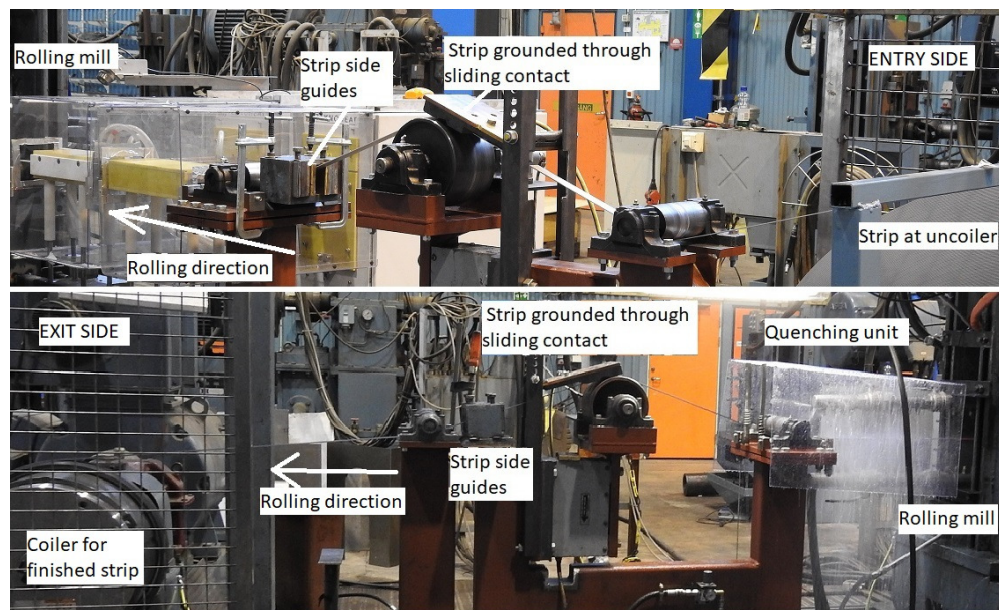


Fig. 16. The actual experimental setup in the MEFOS facilities.



Fig. 17. Quenching unit designed and manufactured by the community for direct quenching (DQ) and direct quenching and partitioning (DQ&P) processes.

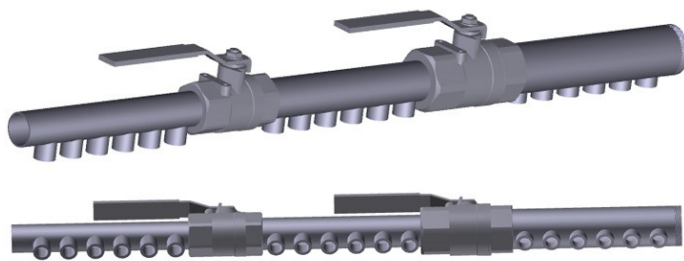


Fig. 18. Quenching unit designed and manufactured by the community for the simulation of DQ and DQ&P.

Additional developments/achievements are listed below:

Temperature logging system

A thermal camera was bought and a temperature logging system (Fig. 19) was developed to enable accurate temperature logging both across and along the strip. The system makes it possible to fully monitor the temperature distribution and follow changes when the target temperature is changed. The positioning of the thermal camera at the entry of the rolling mill is seen in Fig 17.

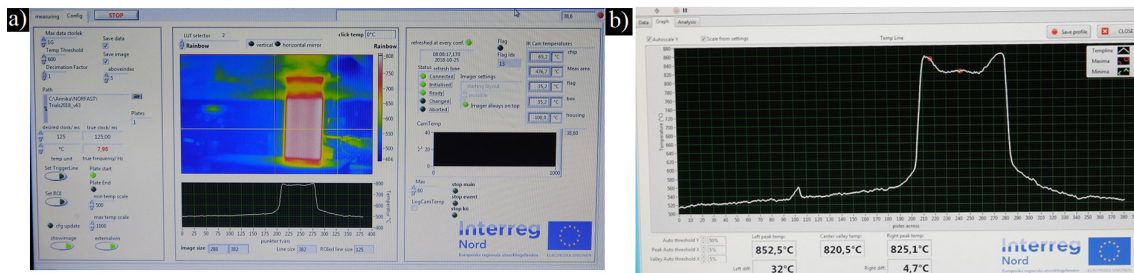


Fig 19. a) Graphical user interface and b) display of the temperature during the trials.

Centering of heater

A motor driven displacement mechanism was developed to be able to center the second inductor depending on the natural equilibrium position of the rolled strip (Fig. 20). This is needed to avoid asymmetric heating and tracking problems. The trials showed that this system was efficient and necessary to reach stable conditions in the line.

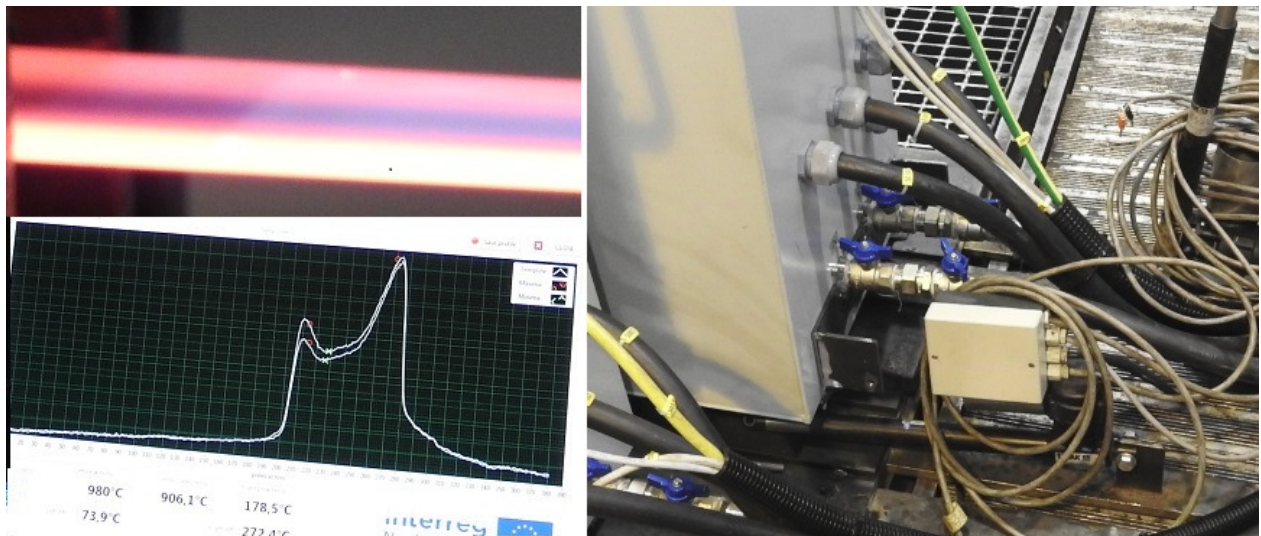


Fig. 20. Asymmetric heating that can be compensated by the electric/mechanic arm unit attached to the heater cabinet.

Strip position control

A monitoring program on image processing (Fig. 21) was made to measure the sideways strip movements during rolling. The purpose was to automatically control the work roll tilt in the case of lateral movements due to wedge shaped conditions or thermal deviations, among others. The control function was not finalized since the function was not needed in NorFaST-HT trials, but the technique is of interest for other types of trials in the mill in the future.

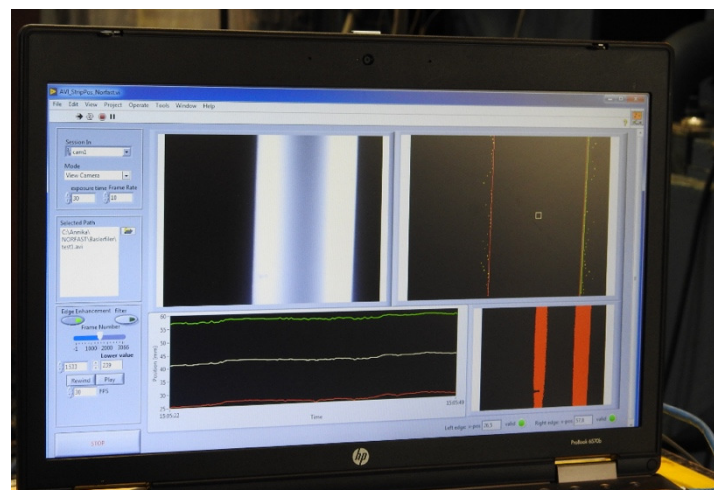


Fig. 21. Graphical user interface - measurement of strip position /control strip steering /mill tilt.

Publications, reports, presentations...

- Jan-Olov Perä, Resistensvärmning av Profil, Norfast-Ht, Försöksrapport829, MEF16091
- John Niska, A review of induction heating and previous research, MEF18062
- Annika Nilsson, Upphandling av induktionsvärmare, MEF18007K
- Annika Nilsson, presentation of the NORFAST project at Rörseminarium 11-12 April 2018 - Högbo Brukshotell, Sandviken



- MEFOS have sent an abstract to ESTAD2019 for presenting the work and results of NORFAST and the induction line as well as the possibilities with heating/rolling /quenching.

1.4 Laser processing laboratory at LTU (Luleå)

At LTU there was a high-power fibre laser with standard processing optics in the beginning of the project. The laser is a 15 kW Yb-fibre laser with a wavelength of 1070 nm. During the project, the intensity profiles and laser beam size were varied through defocusing. A method to predict the microstructure arising from laser heating was developed by utilizing optimized temperature measurements. Thermocouples and a new dual-scope imaging method (a high-speed camera with different filters to record temperature) were used. The test environment is shown in Fig. 22.

The laser lab was updated with a 300 W Yb-fibre laser having the capability to create smaller laser spots and to be used in conjunction with the other laser. In the end of the project, a mirror optics system was acquired to create custom beam shapes by changing one of the lenses. Five different lenses were purchased at the same time. Preliminary testing with the lenses was done in laser hardening processing in the end of the project but the results are not analyzed yet. LTU has also received funding for a 5 kW laser, the procurement process is on-going currently.

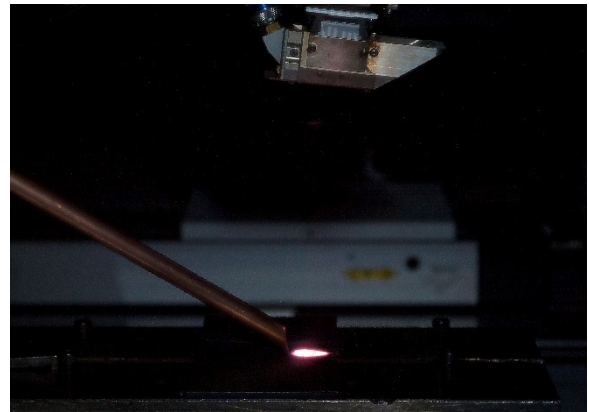
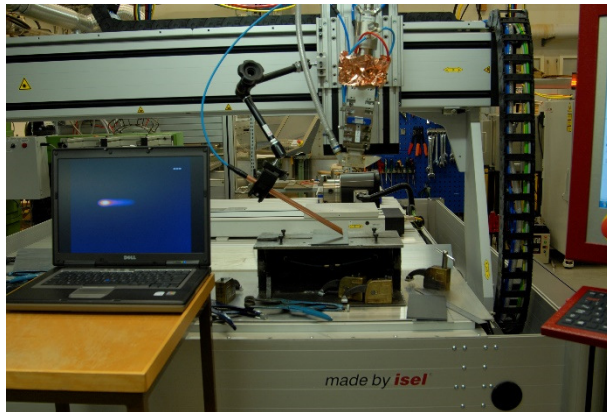


Fig. 22. Experimental setup and trials at the LTU laser laboratory



Chapter 2 – Material technical applications for fast steel heat treatments

- 2.1 Boron alloyed carbon steels – hardening and tempering
 - 2.1.1 Induction processing
 - 2.1.2 Annealing experiments
 - 2.1.3 Hardened structures
 - 2.1.4 Tempered structures
 - 2.1.5 Electric and magnetic properties at high temperatures (B27 boron steel)
- 2.2 Ferritic stainless steels
 - 2.2.1 Thermomechanical simulations of AISI 441
 - 2.2.2 Thermomechanical simulations of AISI 430
 - 2.2.3 Electric and magnetic properties at high temperatures (AISI 430 / 1.4016)
 - 2.2.4 Induction experiments and formability
- 2.3 Austenitic stainless steels (301LN)
 - 2.3.1 Tensile strength
 - 2.3.2 Cyclic strength
 - 2.3.3 Formability
 - 2.3.4 Weldability issues
 - 2.3.5 Electric and magnetic properties at high temperatures (AISI 301LN / 1.4318)
- 2.4 Special processes and applications
 - 2.4.1 Post treated welded joints
 - 2.4.2 Surface hardened ferritic stainless steel AISI 410L (1.4003)
 - 2.4.3 Drop-deposit additive manufacturing with a common laser source

Publications, reports, presentations...

- ADVANTAGES OF FAST (INDUCTION) HEAT TREATMENT - Where and Why ?: Presentation on general aspect (Prof. Pentti Karjalainen)

2.1 Boron alloyed carbon steels – hardening and tempering

2.1.1 Induction processing

Induction heating can be used for hardening and tempering similarly as any other heat source. Induction hardening has been traditionally applied to the surface hardening process. Heat is created at a shallow surface layer of a steel workpiece and rapid cooling or even self-cooling (heat conduction to untreated parts of the workpiece) hardens the structure. Surface hardening is typically a very fast heat treatment, i.e. both the heating and cooling rates are high. Hardness values of 2–4 HRC higher than in conventional processing have been commonly reported. This so-called super hardness is not clearly understood, and its origin has not been established, but it can be attributed to several factors including residual stresses and final microstructure (carbide shape and density, retained austenite, dislocation density of the martensitic matrix, grain size, among others) [1-3]. Fine-grained, homogeneous normalized prior-structures, as well as quenched and tempered structures have more chance to exhibit super-hardening contrary to surface hardening, through hardening of a steel sheet, e.g. for bulk steel manufacturing, is technologically more challenging. It is difficult to heat a wide variety of large sheets homogeneously to austenitizing temperatures. Inductor is typically fixed for a constant sheet width limiting the commercial applications.

Induction tempering of hardened carbon steels is technologically much easier. A single axial flux inductor is suitable for tempering wide variety of products without need to fix the dimensions so tightly. The efficiency is relatively high (> 90%) along the whole temperature range (below the Curie-point). The novel idea presented in



this project is to develop a surface tempering process to manufacture enhanced steel grades with reduced costs.

2.1.2 Annealing experiments

During the NorFaST-HT -project, induction hardening tests were carried out using all three heating facilities located at Nivala, Lund and Luleå. The Nivala line (Section 1.1) is based on 600 kW axial flux inductor (MP600) making it suitable for various specimen dimensions, but the inductor has limited efficiency beyond the Curie-point (Fig. 23a). The MP600 is not very sensitive to vertical centering of the test samples due to the inductor type, making it flexible for studying various processes. The edges of the test samples are slightly overheated and not used for material characterization. Due to the properties and performance of the MP600 inductor, it was also used for tempering and reversion experiments.

“Laboratory unit” at Lund (Section 1.2) is based on a 70 kW transversal flux inductor providing a high efficiency beyond the Curie-point (Fig. 23b). This unit was used to produce reference data with enhanced performance in hardening processes. As can be seen by comparing Figs. 23a and b, the “Laboratory unit” provides almost a linear heating rate over the whole temperature range while the MP600 unit shows a significantly reduced heating rate beyond the Curie-point. The lower efficiency of the MP600 unit decreases the line speed (sheet feed) and the low line speed is, in turn, seen as a low initial cooling rate before the sheet reaches the quenching nozzles (the distance approximately 25 cm between the inductor and the quenching unit). It is concluded from the literature survey (Report “HARDENABILITY OF A Mo-B-BEARING STEEL AFTER INDUCTION HEATING”) that a low initial cooling rate (less than about 15 °C/s) tends to decrease the hardenability of Mo-B bearing steels due to boron carbide precipitation. The optimum B-content is about 9 ppm (0.25%Mo) and the excess increases the risk of harmful precipitation. To simulate rapid quenching (immediately after annealing), a special solution was developed for the “Laboratory unit” to transfer the test specimen quickly to the quenching tank. As seen from Fig. 23b, there is no self-cooling stage before quenching.

The third research facility, the “MEFOS line”, offers a unique possibility to run real continuous production simulation with hot rolling. The “MEFOS line” operates at fully continuous mode so it is difficult to measure temperature from a single spot to record the temperature history. The maximum temperature is determined with a thermal camera using a line measurement as shown in Fig. 24. The example temperature curve is produced using the coil no. 2 that caused quite non-uniform temperature distribution along the width of the sheet.

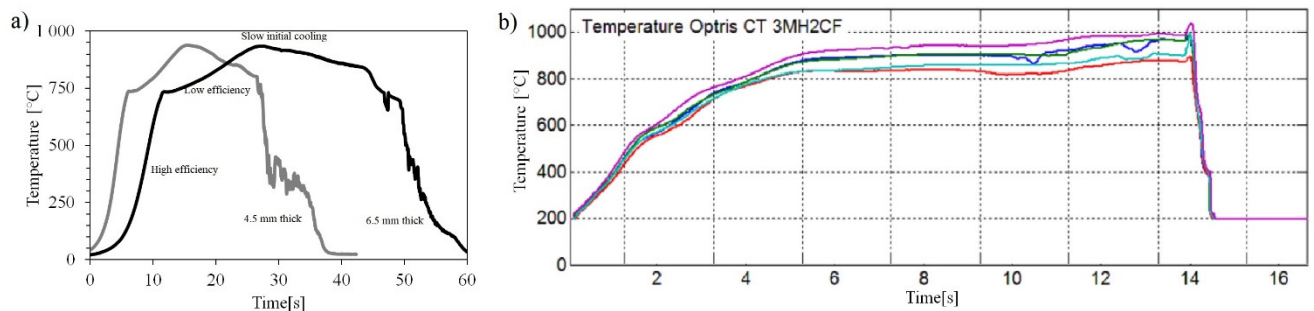


Fig. 23. Temperature measurement results from induction hardening experiments showing a) MP600 performance with 4.2 (1.3 m/min) and 6.5 mm (0.75 m/min) thick B27 boron steel (thermocouples) and b) “Laboratory unit” performance with 2.0 mm thick B24CR steel (pyrometer).

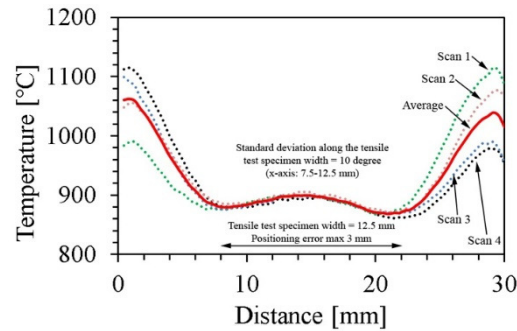


Fig. 24. Temperature distribution in continuous annealing without hot rolling using 2 mm thick B24CR steel with Coil Design v.2. The average temperature in the center is approximately 890 °C.

Publications, reports, presentations...

- *Induction heating for heat treatment of steel plates: Lund/MagComp analysis on industrial equipment and investment costs*
- **HARDENABILITY OF A Mo-B-BEARING STEEL AFTER INDUCTION HEATING:** Literature survey and discussion on the effect of processing conditions on hardenability of boron steels (Prof. Pentti Karjalainen)

2.1.3 Hardened structures

Hardened specimens were mechanically tested using hardness and tensile testing. Microstructural analyses were carried out using optical microscopy to determine the prior austenite grain sizes (PAGSs). One of the main objectives was to refine the PAGS to increase the strength without impairing the ductility. Test materials were mainly B24CR and B27 boron steel grades, although 22MnB5 and 30MnB5 grades were also briefly studied. Only the selected results are presented in this report.

Hardened B27 grade (Nivala induction line, MP600). The reference wear resistant steel, commercial MX500 (press hardened B27 grade from Miilux Company), showed approximately 30 μm PAGS (Fig. 25a) and ultimate tensile strength (UTS) of 1786 MPa with approximately 7% total elongation (TE) until fracture. The induction hardened B27 counterparts showed significantly smaller PAGS of 5–10 μm (Fig. 25b) and almost 100 MPa higher UTS (Fig. 26a). Smallest PAGS were obtained by heating just above the A_{c3} temperature (820 °C). The heating rate above the Curie-point was approximately 10–25 °C/s depending on the annealing temperature and sheet thickness. Similar prior austenite structures were achieved in reference tests carried out using a Gleeble simulator as shown in Fig. 25c. The yield strength was consistently lower in induction hardened specimens than in the commercial grade. Total elongation (Fig. 26b) was equal in the MX500 and induction hardened 4.5 mm thick B27 steels, but slightly poorer ductility was observed with the thicker B27 sheet. The increase in the sheet thickness decreases the line speed in continuous annealing to reach the same temperature with the same sheet width. Since the distance between the inductor and quenching unit is fixed, the self-cooling stage is longer in the instance of thicker sheets (e.g. black curve in Fig. 23a), indicating that the delayed quenching (slow self-cooling) tends to impair the ductility in the continuous induction hardening process.

The effect of annealing temperature, holding time and cooling rate were briefly studied using a Gleeble simulator for annealing experiments and hardness testing for material characterization. The simulation results (Fig. 27) are consistent with induction hardening results (Fig. 26). The annealing temperature only has a slight effect on the average hardness as it has on UTS when the annealing temperature was clearly above the A_{c3} temperature (820 °C). In the Gleeble experiments, hardness already saturated at around 850 °C, while in induction experiments a higher temperature of approximately 50 °C was needed. The difference may be caused by the measurement errors caused by the magnetic fields or due to different processing conditions. Based on the Gleeble simulations (Fig. 27b), the increase in cooling rate does not increase the hardness, but it must be at least 10 °C/s for martensite transformation. Similarly, the increase in quenching pressure in the range of 1.5–10 bars did not affect the hardness in induction hardening.

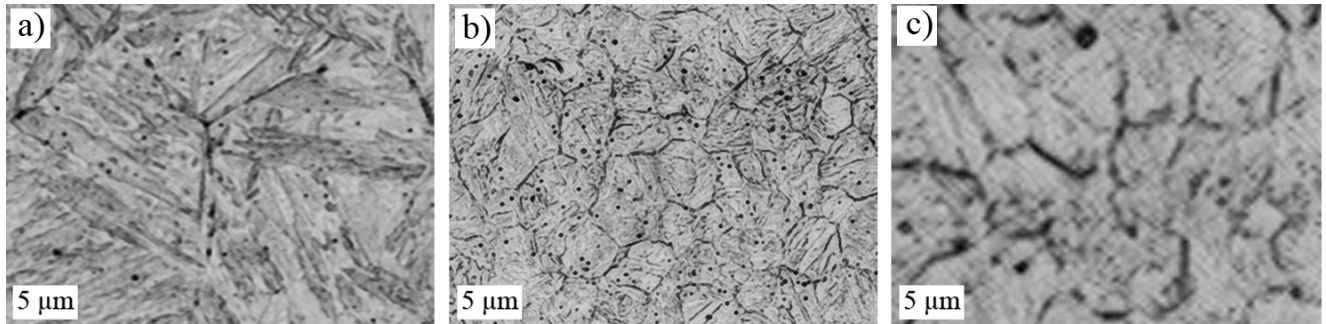


Fig. 25. Prior austenite grain structure for a) commercially hardened B27, b) induction hardened B27 (MP600) and c) Gleeble hardened B27.

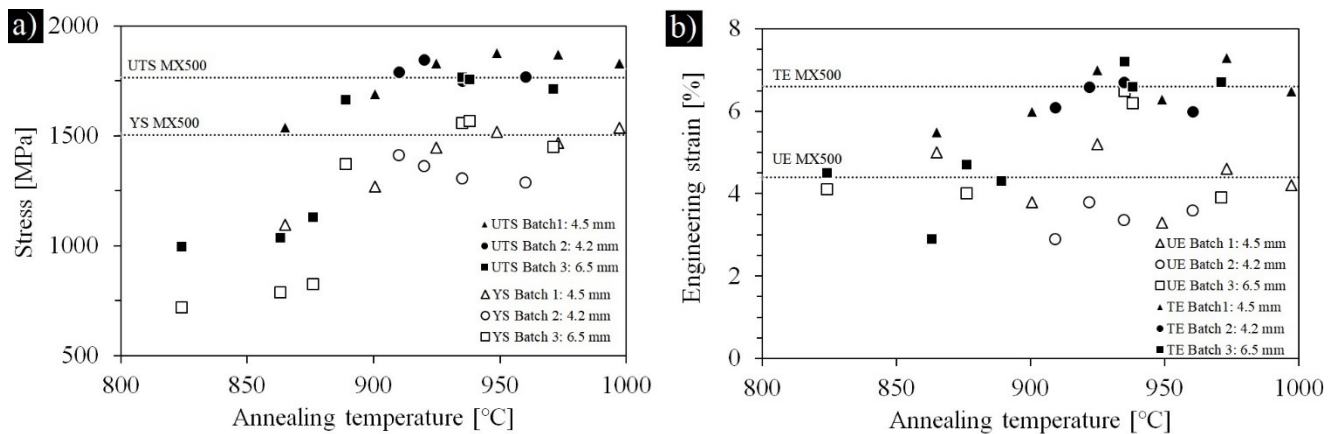


Fig. 26. a) Tensile strength and b) elongation for induction hardened B27 steel after annealing (MP600) at various maximum temperatures followed by water quenching. MX500 = commercial Milux 500 steel grade. Sample size in annealing experiments 4.2–6.5 x 400 x 1000–2500 mm (t x W x L) and in tensile tests 12.5 x 50 mm (W x L, gauge section).

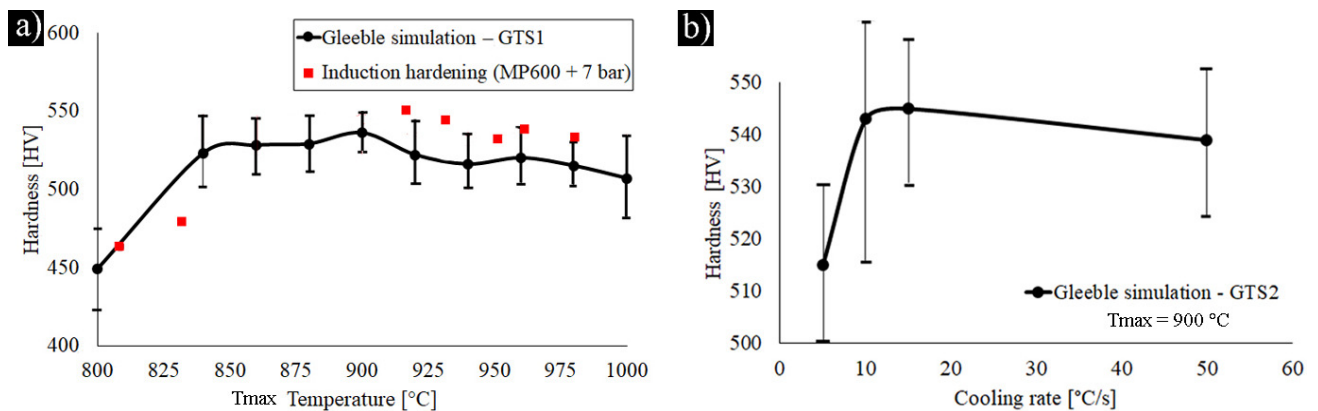


Fig. 27. Average hardness of the Gleeble hardened B27 steel showing the effect of a) annealing temperature (red squares showing induction hardened counterparts) and b) cooling rate. Sample size in annealing experiments 4.5 x 10 x 50 mm (t x W x L).

Hardened B24CR grade. Both the “Laboratory unit” at Lund and new induction line in SWERIM facilities were used for induction hardening experiments of 2 mm thick B24CR steel. Reference tests were carried out earlier in Oulu using a conventional furnace and water quenching and in Nivala using laser heating and additional water quenching. In the induction experiments, few different maximum temperatures were applied with the “Laboratory unit”, but the SWERIM line had a limitation in the maximum temperature so only the highest annealing temperature is shown in Fig. 28. The tensile strength was quite independent of the manufacturing route, but finer grain sizes were observed with induction and laser hardening. The elongation was slightly enhanced due to grain refinement.

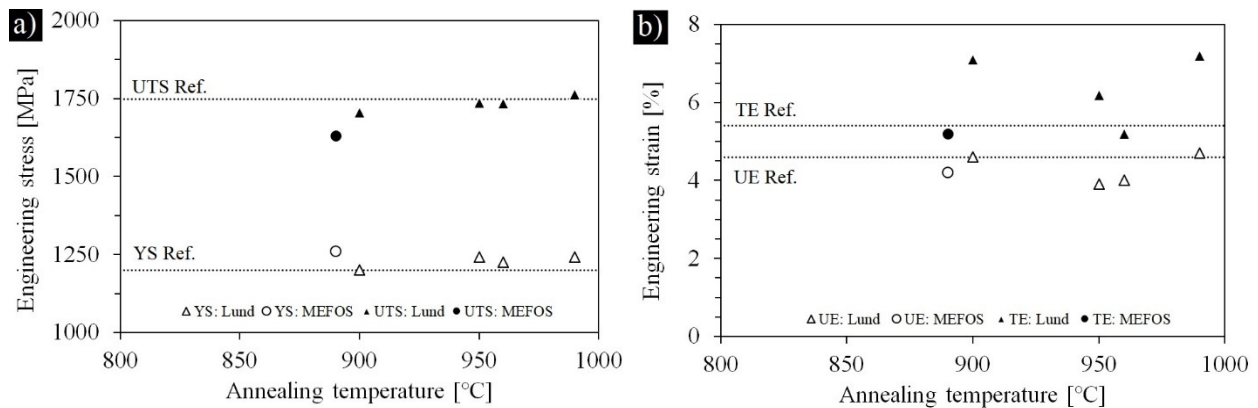


Fig. 28. a) Tensile strength and b) elongation for induction hardened B24CR (2 mm) steel after annealing (MP600) at various maximum temperatures followed by water quenching. Ref. water quenched (from 925 °C) B24CR. Sample size in annealing experiments in Lund 2 x 114 x 500 mm (t x W x L), in MEFOS 2 x 30 x 5000 mm (t x W x L) and in tensile tests 12.5 x 50 mm (W x L, gauge length).

In summary, Table 1 lists selected tensile test properties for various steel grades studied. Induction hardening experiments showed that the tensile properties after fast annealing and quenching are at least equal or even better than the ones of slowly annealed and quenched counterparts. To increase the strength, hardening process can be repeated to refine the PAGS furthermore. For example, induction hardened structure (949 °C) was annealed again at various temperatures from 800 to 1000 °C. Tensile strength was consistently higher than observed without the repetition. The same process was also implemented for a commercially hardened MX500 grade. Even though the UTS of the MX500 was lower than with the induction hardened counterpart, both structures reached the UTS of 1930 MPa after the second hardening treatment. Rough estimation was that the mechanical properties were more homogenous in the doubled hardened MX500. The PAGS after second hardening stage was approximately 3 μm.

Table 1. Tensile property comparison between different grades and manufacturing routes. * [4]

Grade	Hardening route	T _{max} [°C]	UE	TE	YS	UTS
				[%]		[MPa]
B24CR	Conventionally hardened	925	4.6	5.4	1200	1748
B24CR	Induction hardened	990	4.7	7.2	1243	1763
B27	Commercial press hardened	-	4.4	6.6	1505	1767
B27	Induction hardened	949	3.3	6.3	1517	1880
B27	Induction hardened twice	949 + 865	2.7	5.9	1588	1937
30MnB5	Induction hardened	910	6.0	7.0	1544	1840
30MnB5	Laboratory press hardened*	900	4.1	6.7	1262	1855

Publications, reports, presentations...

- *Induction heating for heat treatment of steel plates:* Lund/MagComp analysis on industrial equipment and investment costs
- **HARDENABILITY OF A Mo-B-BEARING STEEL AFTER INDUCTION HEATING:** Literature survey and discussion on the effect of processing conditions on hardenability of boron steels (Prof. Pentti Karjalainen)



2.1.4 Tempered structures

Fast induction tempering of a hardened B27 steel (MX500) was studied preliminary in the RPST-project (2012–2014). The mechanical properties of induction tempered (Nivala line) B27 structures were presented in a conference paper [5] showing that tensile properties and bendability of rapidly tempered structures are at least as good as the conventionally tempered structures. During the NorFaST-HT -project, new trials were carried out for SSAB prototype steel grades, direct quenched (DQ) at the Raahe factory and induction tempered in Nivala. Also some new trials were carried out for hardened boron steels.

Induction tempering. The motivation for study is to clarify the advantages of fast tempering. In a recent martensite strength model of Galindo-Nava and Rivera-Díaz-del-Castillo [6], the strengthening mechanisms in the martensitic structure include three factors: high-angle grain boundary strengthening (“grain” size), increase in the dislocation density, and carbide precipitation; the latter becoming active during tempering. Fast tempering cycles offer some opportunities for microstructure control, e.g. by carbide size and distribution, dislocation density and ferrite grain size [7,8]. The earlier results [4,9] have showed that fast induction tempering can be applied to produce identical tensile properties and bendability for various steel alloys than observed with conventional “slow” tempering. On the other hand, induction hardening experiments have revealed significant grain refinement, so the final induction hardened and tempered structure could benefit from the both processes. For example, Judge et. al. concluded that Q&T processing leads to enhanced toughness properties of martensitic carbon steel [10].

Tempering example Case 1. The 8 mm thick test material (coded as DQ&T1100) was tempered above 600 °C using the Nivala induction line. The target temperature (P-value ~17) was over 700 °C in contrary to the reference tests carried out conventionally at 650 °C for 15 minutes (same P-value). The heating rate was approximately 150 °C/s. Due to some technical reasons, the air curtain had to be used during some tests and the effect of the air flow is seen in Fig. 29 as discontinuous cooling during ~5 seconds after the heating ends. The dotted line in the figure shows a smooth curve when test was repeated without the air curtain (reversed operation mode, Fig. 30). The maximum surface temperature was limited to the Curie-point with the selected line speed range. Increase of the line speed to approximately 3.2 m/min showed the first clear decrease in the annealing temperature. Material characterization results were in agreement with the earlier observations. Tensile properties were similar as in the reference structures created in the SSAB research laboratory, but an enhancement in the impact toughness was observed in induction tempered counterparts. With some steel grades, the enhancement is significant enough to increase the impact toughness to accepted levels which were not reached by other means.

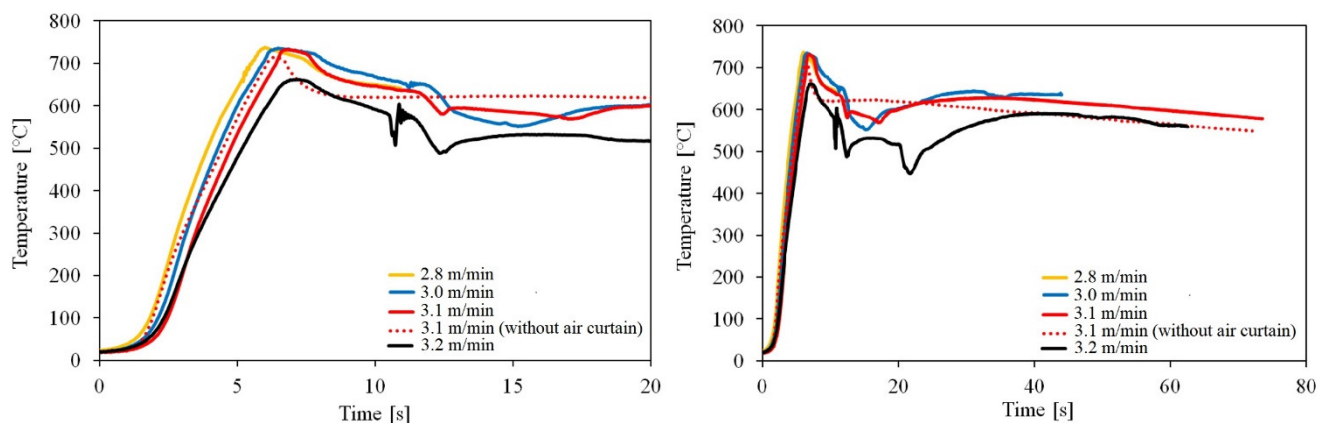


Fig. 29. Temperature measurement results for induction tempering tests in Nivala (MP600). Sample size in annealing experiments 8 x 400 x 1500 mm (t x W x L).

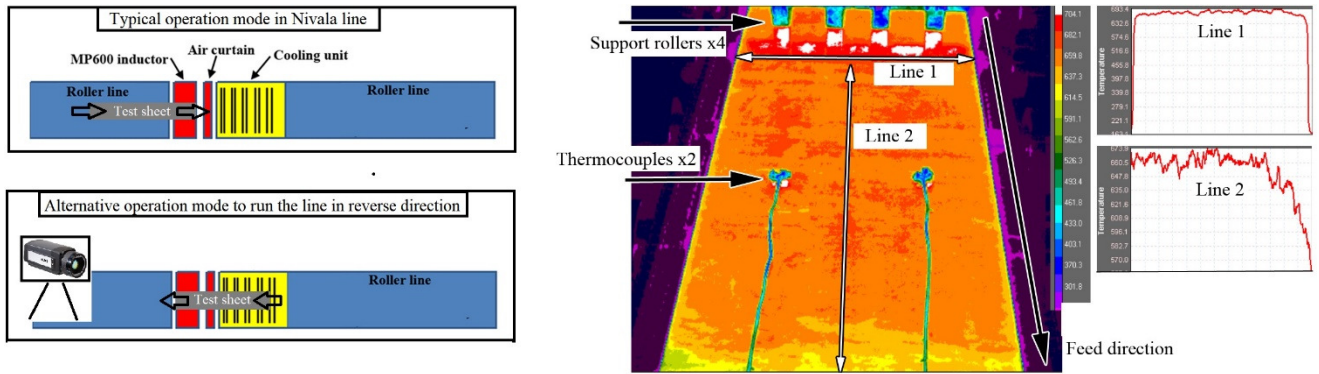


Fig. 30. Thermal imaging during induction tempering of 8 mm 1100 DQ&T. The line was running in reversed direction to allow the use of thermal camera and also to prevent air curtain to cool the surface of the sheet.

Tempering example Case 2. The 600 HBW wear resistant steel has relatively low-toughness microstructures. For example, the press-hardened B40S steel fulfills its impact toughness requirements only in thick plate products. Thinner (e.g. < 10 mm thick) plates exhibit typically lower impact toughness than the thicker products do and some of them are not valid for commercial sales. The effect of low-temperature induction tempering on impact toughness was studied during the NorFaST-HT -project. As seen in Fig. 31a, the impact toughness was enhanced in the low-temperature tempering, but the absolute level remained poor. The enhancement was, however, more efficient with induction than with conventional tempering. For example, tempering at approximately 200 °C increased the impact toughness (at -40 °C) 30% and 10% with induction and conventional tempering, respectively. To reach the impact energy of 27 J at -40 °C, tempering had to be carried out at high temperatures resulting in too severe softening for practical wear applications.

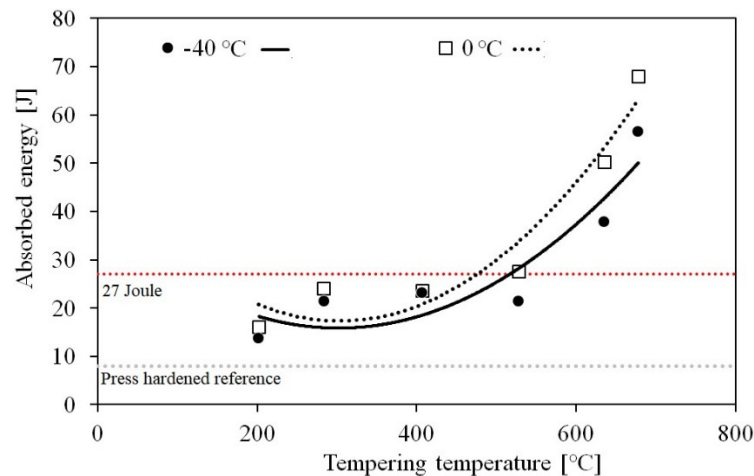


Fig. 31. The effect of fast induction tempering on impact toughness (transversely to the rolling direction) of press hardened 8 mm thick B40S steel.

Publications, reports, presentations...

- Induction heating for heat treatment of steel plates: Analysis on industrial equipment and investment costs (Lund/MagComp)
- A steel for effective utilization of high rate (induction) heating and low-temperature tempering: Literature survey and discussion on fast (low-temperature) tempering (Prof. Pentti Karjalainen)

2.1.5 Electric and magnetic properties at high temperatures (B27 boron steel)

The B27 boron steel is a common hardenable low alloyed carbon steel (nominal composition shown in Table 2). The trademarks of SSAB for similar products are based on the carbon content, e.g. B24 has the nominal



carbon content of 0.24%. Similar standardized alloys are for example 20MnB5 (EN 1.5530) and 38MnB5 (EN 1.5532) where the number before Mn stands for the carbon content. Other commercial trademarks are for example MBW 1500 +AS (ThyssenKrupp) and Usibor 1500P (ArcelorMittal).

The measured electromagnetic properties behave as one would expect, i.e. the B-H (Fig. 32a) is getting smaller while the temperature increases. Although this is an expected behavior, the absolute values are often hard to approximate with any degree of accuracy, especially when requiring temperature dependency. The absolute values of the measured properties are useful when, for instance, dimensioning or simulating an induction heater. In this case the resistivity (Fig. 32b) and the relative permeability (Fig. 33) are perhaps the most useful properties.

Table 2. Nominal chemical composition of the alloy (in wt%).

C	Mn	Si	Cr	Ti	B	Fe
0.27	1.2	0.25	0.3	0.04	0.002	Bal.

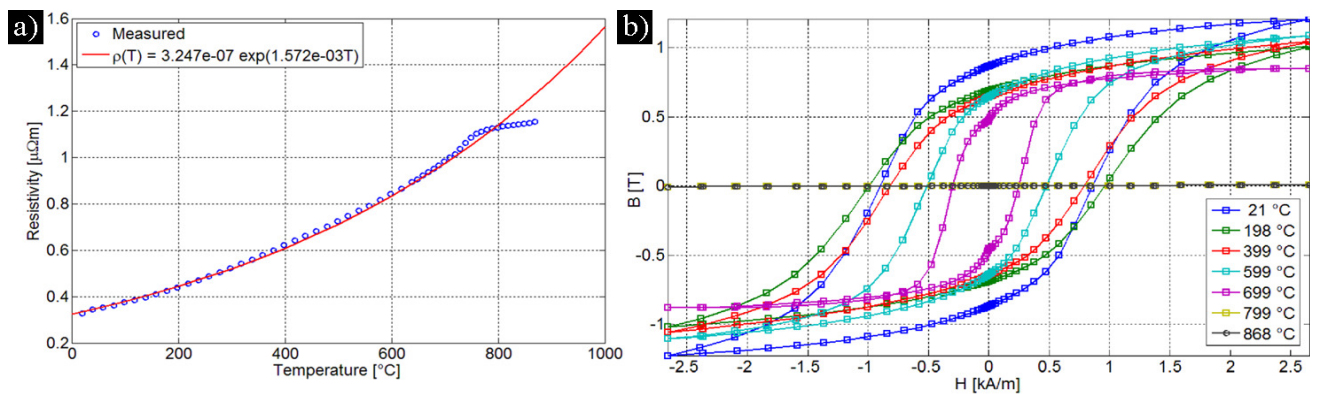


Fig. 32. (a) Measured resistivity (blue circles) and parametrized temperature dependency of the resistivity (red line) and (b) full hysteresis loops with $H_{peak} = 2656$ A/m.

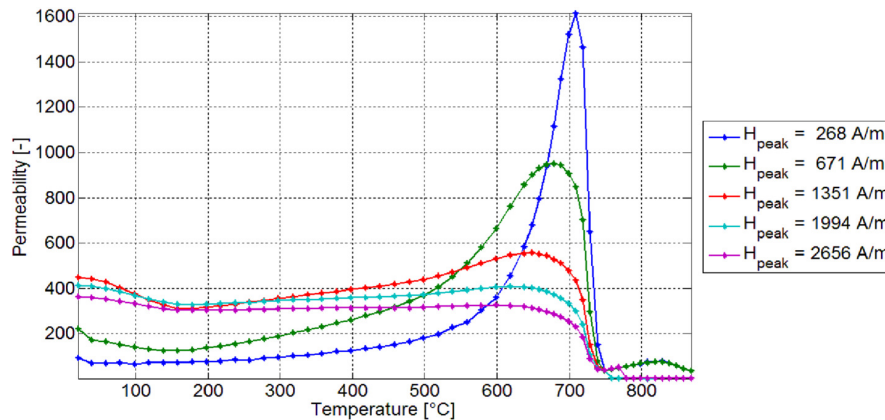


Fig. 33. Measured temperature dependency of the permeability at peak magnetic flux density.



Publications, reports, presentations...

- “Electric and Magnetic Data for B27, Boron steel, SSAB/Rautaruukki”: Physical properties for the boron steels (Lund). Electric and Magnetic high temperature data for 1.4016

References for Chapter 2.1

1. Valery I. Rudnev, FASM, Inductoheat Group, Metallurgical insights for induction heat treaters, HEAT TREATING PROGRESS • Sept., 2008, 35/.
2. S. Sackl, H. Leitner, M. Zuber, H. Clemens, S. Primig, Induction Hardening vs Conventional Hardening of a Heat Treatable Steel, Metall. Mater. Trans. A 45 (2014) 5657-5666 doi: 10.1007/s11661-014-2518-4
3. S. Papaefthymiou, V. Karamitros, M. Bouzouni, Ultrafast Heating and Initial Microstructure Effect on Phase Transformation Evolution of a CrMo Steel, METALS 9 72 (2019), doi:10.3390/met9010072
4. J. H. Lee, Y. R. Cho, S. D. Choo, Tensile Properties and Bendability of B-bearing Martensitic Steels, May 21st – 23rd 2014, Brno, Czech Republic
5. A. Järvenpää, J. Lämsä, E. Patard, K. Mäntyjärvi, A Novel Heat Treatment Line for Processing of Tailored Small Batch Steels, Key Eng. Mat. (2014) 611-612, 804-810
6. E.I. Galindo-Nava, P.E.J. Rivera-Díaz-del-Castillo, Acta Mater. 98, 2015, 81–93
7. S. Shackl, M. Zuber, H. Clemens, S. Primig, Induction Tempering vs Conventional Tempering of a Heat-Treatable Steel, Met. Mat. Trans. A 47 (2016) 3694-3702 doi:10.1007/s11661-016-3534-3
8. C. Revilla, B. Lopez, J.M. Rodriguez-Ibabe, Carbide size refinement by controlling the heating rate during induction tempering in a low alloy steel, Mat. Design 62 (2014) 296-304
9. A. Saastamoinen, A. Kaijalainen, D. Porter, P. Suikkanen, The effect of thermomechanical treatment and tempering on the subsurface microstructure and bendability of direct-quenched low-carbon strip steel, Mater. Charact. 134 (2017) 172-181
10. V.K. Judge, J. G. Speer, K. D. Clarke, K. O. Findley, A. J. Clarke, Rapid Thermal Processing to Enhance Steel Toughness, Scientific Reports 8 (2018) 445

2.2 Ferritic stainless steels

Low-carbon ferritic stainless steels are cost-effective alternatives for austenitic stainless steel grades, because ferritic grades do not contain any expensive nickel. The most important feature in the stainless steels is not only their corrosion resistance, but also their formability. For example, the automotive industry is interested in new possibilities of using modern and future stainless steels in their products. Use of stainless steels would reduce e.g. the need of painting and galvanization.

The NorFaST-HT -project focused on studying the effect of heating rate on microstructural features affecting the formability. It has been shown earlier by Muljono et al. [1] and more recently by Massardier et. al. [2] that the increase in the heating rate (up to 200 °C/s) promotes the formation of {111}<uvw> texture in ferritic steels. Same trend has also been recorded for stainless steels [3,4], and this texture (strong gamma fiber) is known to enhance the deep-drawing abilities of low-carbon (0.003–0.05 %C) ferritic steels [2,4-7]. High heating rate inhibits the diffusion of carbon from carbides and increases the number of nuclei of favorable texture components [8]. The main research question in the NorFaST-HT -project was if the texture can be strengthened similarly also in ferritic stainless steels. Secondly the effect of processing parameters on grain structure and mechanical properties were studied.

To study the effect of the heating rate on {111}<uvw> texture, two cold rolled (~80%) test materials (AISI 441 and 430 type steels) were annealed using a Gleeble simulator and also a MP25 inductor with the sheet support system shown in Fig. 6 (Chapter 1). Annealed specimens were characterized using XRD, FESEM-EBSD and tensile testing.

2.2.1 Thermomechanical simulations of AISI 441 (1.4509)

Annealing. Sheet pieces of 10 x 50 mm, cut parallel to the rolling direction, were heated on a Gleeble 3800 simulator at the heating rates of 25 and 500 °C/s to annealing temperatures of 950, 1050 and 1150 °C. Isothermal holding of 10 s was applied followed by cooling at the rate of 35 °C/s to room temperature. Finally, pieces of 150 x 20 mm were cut parallel, 45° or transverse to the rolling direction and heated to 1050 °C at 25 and 500 °C/s, using the same holding time of 10 s and cooling rate of 35 °C/s for tensile testing.



Grain structure. The results were consistent with earlier experiences showing an increase in the grain size with increasing the annealing temperature. On the other hand, increasing the heating rate decreases the grain size due to more effective nucleation of new grains at the beginning of recrystallization. As seen from Fig. 34, the grain structure is much finer in the structure annealed at 500 °C/s to 950 °C than in the reference structure simulating the heating condition in industrial conditions with the conventional annealing facility. For formability, the grain size should be relatively coarse (~20–30 μm). At higher annealing temperatures, the difference in grain sizes between the heating rates was modest. The grain size of approximately 35 μm was achieved using both heating rates to 1050 °C.

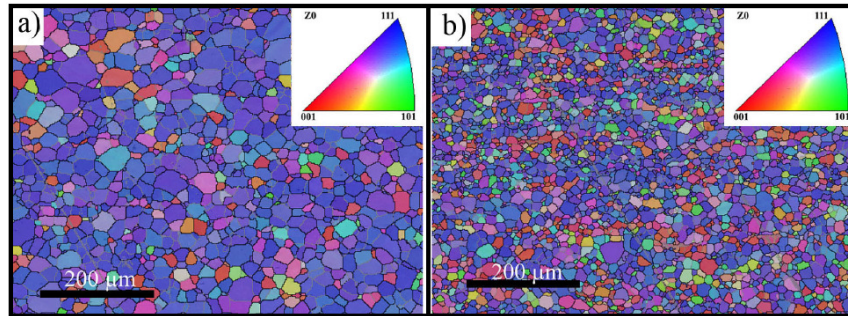


Fig. 34. Cross-sectional microstructure of a specimen heated to 950 °C at 25 °C/s for 10 s (a) and 500 °C/s (b) showing clearly finer fully recrystallized grain structure in rapidly annealed structure.

Texture. All annealing experiments resulted in the near gamma-fiber recrystallization texture, which is consistent with the results in previous studies. For example, Sinclair et al. [8] presented that nuclei having the gamma-fiber orientation nucleate and grow very fast at the beginning of the recrystallization, and they consume surrounding grains. In the present experiments the gamma-fiber intensities were high already in the commercial base material. In the subsequent annealing experiments, the high heating rate led to slightly enhanced gamma-fiber intensities. However, the specimen heated at 500 °C/s to the lowest temperature of 950 °C, the time for the grain growth remained relatively short and all grains did not have the gamma-fiber orientations, which led to a lower texture intensity.

Formability based on tensile testing. The both specimens heated at 25 or 500 °C/s to 1050 °C exhibited practically equal R-values. This is consistent with the texture measurements, as the both specimens had slightly enhanced texture intensities in the gamma-fiber. At this point it can be noted that even though the influence of the heating rate on the formability (deep drawability) of the sheet appeared to be negligible, relatively high R-values could be achieved through the rapid thermal cycle utilizing the high heating rate. Erichsen cupping test results are presented together with the AISI 430 in Section 1.2.4.

Publications, reports, presentations...

- M. Jaskari, A. Järvenpää, L.P. Karjalainen, The Effect of Heating Rate on Texture and Formability of Ti-Nb Stabilized Ferritic Stainless Steel, Key Eng. Mater. 786 (2018) 3-9

2.2.2 Thermomechanical simulations of AISI 430 (1.4016)

Annealing. Cut pieces of 10 x 50 mm were subsequently heat treated on a Gleeble 3800 simulator at the heating rates of 25 or 500 °C/s. The annealing temperature was varied between 830 and 950 °C. The holding time 10 s and the constant cooling rate 35 °C/s to room temperature were applied.

Grain and phase structure. The results were slightly different from those with AISI 441. The average grain size increased similarly with the annealing temperature, but the heating rate did not affect the grain size so clearly. It can be noted that the complete recrystallization has already occurred even in annealing at the lowest peak temperature of 830 °C with the heating rate of 500 °C/s. The ferrite grain size was quite fine (clearly finer than in AISI 441), and only very limited grain growth could take place, because of low annealing temperature in



the ferritic region and a short holding time of 10 s. Furthermore, the grain size was slightly smaller with specimens heated at 500 °C/s, which indicates more effective nucleation during the start of recrystallization, as proposed by the literature, e.g. [1,8], although the differences remained small. The formation of austenite at 925 °C and above prevented the heating to higher temperatures, for the presence of austenite led to the formation of martensite. The specimen heated to 830 °C or to 900 °C had almost the equal hardness, 152 HV5 on the average. Specimen heated to the intercritical temperatures of 925 °C or 950 °C had a higher hardness, 154 and 181 HV5, while heated to 925 °C at 25 °C/s and 500 °C/s, respectively. The increasing hardness indicates the formation of austenite during soaking and martensite during cooling. The presence of martensite in addition to ferrite and carbides is seen in Fig. 35, the amount depending on the annealing temperature.

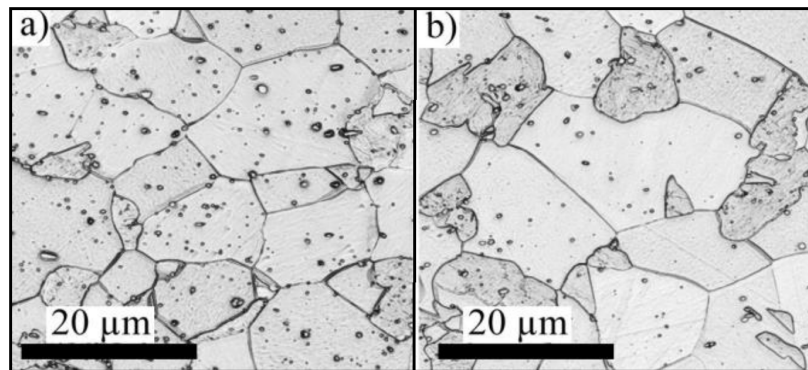


Fig. 35. Grain structure of a specimen heated at 500 °C/s and annealed for 10 s at (a) 925 °C and (b) 950 °C showing ferrite and martensite (darker grains) and chromium carbides.

Texture. The recrystallization texture was typical of annealed ferritic stainless steel in all studied specimens and the improvement of the gamma-fibre texture due to the high heating rate annealing seems to be quite marginal. This can be explained by the short annealing time and low annealing temperatures. The limited grain growth prevents the excess formation and growth of the new grains having the near {111}<uvw> gamma-fibre orientations. However, using a short annealing cycle with a high heating rate was found to provide a relatively high gamma-fibre texture, which is known to be beneficial for the formability.

Formability based on tensile testing. Using the high heating rate led to practically equal tensile properties to those of the slowly heated counterpart, and slightly increased R-values, which might indicate enhanced formability properties.

Publications, reports, presentations...

- M. Jaskari, A. Järvenpää, L.P. Karjalainen, The Effect of Heating Rate and Temperature on Microstructure and R-value of Type 430 Ferritic Stainless Steel, *Mat. Sci. Forum* 943 (2018), pp. 364-369

2.2.3 Electric and magnetic properties at high temperatures (AISI 430 / 1.4016)

AISI 430 (1.4016) ferritic stainless steel (nominal composition shown in Table 3). The UNS, JIS and ISO codes are S430000, SUS 430 and 4016-430-00-1, respectively. In comparison to conventional austenitic stainless steels, the crystal structure in room temperature is body-centered cubic structure. This has a significant effect on electric and magnetic properties.

The electromagnetic properties are, again, behaving more or less as expected. One thing that stands out in the results is the Curie point, which occurs at around 670 °C. This is seen in Fig. 36 when the relative permeability goes down to one. This is lower than one would normally approximate for a ferromagnetic steel. However, different alloying elements and lattice structures may affect the Curie temperature and it is well within reasonable range.

In comparison to the austenitic stainless steels discussed in section 1.1.3, this is much easier to induction heat while maintaining high efficiency. The resistivity (Fig. 36) is significantly lower than for the austenitic grades, requiring higher current intensity to match the heating power. This is compensated by the high relative



permeability which compresses the induced current into a smaller cross-sectional area, given the same process parameters.

Table 3. Nominal chemical composition of the alloy (in wt%).

C	Mn	Si	Cr	P	S	Fe
<0.04	<1.00	<1.00	16–18	<0.04	0.015	Bal.

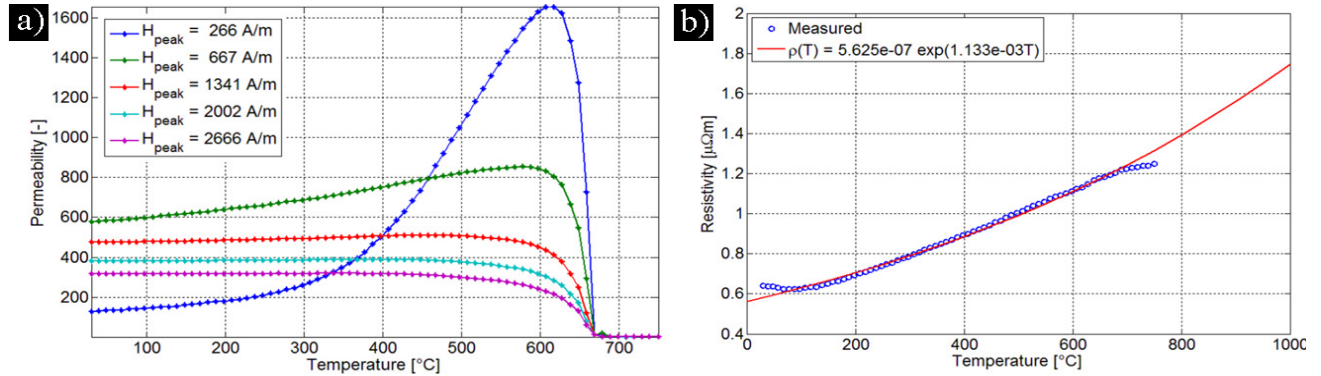


Fig. 36. (a) Measured temperature dependency of the permeability at peak magnetic flux density and (b) measured resistivity (blue circles) and parametrized temperature dependency of the resistivity (red line).

Publications, reports, presentations...

- “Electric and Magnetic Data for AISI 430 (1.4016)”: Physical properties (Lund).

2.2.4 Induction experiments

Induction annealing experiments were carried out in Nivala using a MP25 power source and face-inductor (active coil size 10 x 200 mm) together with the developed sheet support system (Fig. 6). The coil was placed in approximately 45° angle towards the sheet. Even though new support system was built, there still existed severe thermal bending (higher tension stress required) causing temperature differences in test pieces (size 200 x 1000 mm). Most homogenous regions of heated pieces (size of 50 x 200 mm) were selected for preliminary tensile and Erichsen cupping tests and the results were compared with similarly tested commercial and Gleeble-treated test pieces.

The formability results (Fig. 36) are based on the limited data on narrow specimens (similar condition for all specimens). In comparison to the commercial AISI 430 and 441 steels, the quickly annealed counterparts showed lower yield strength (YS) and higher Erichsen index (IE). 11% decrease in YS increased the IE by 20% for 430 steel. Similarly 5% decrease in YS increased the IE by 10% for 441 steel. The YS comparison is made using the highest measured YS. The scatter in IE was high especially with the induction annealed structures. This is obviously related to annealing conditions.

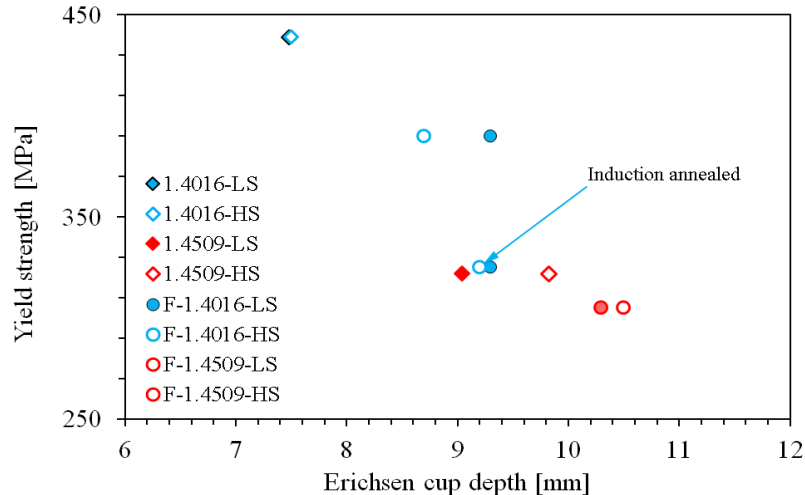


Fig. 36. The Erichsen index in relation to yield strength for AISI 430 and 441 steels both in commercial and laboratory annealed conditions (coded F-xxx). Punch speeds of 0.5 mm/s (LS) and 100 mm/s (HS) were used. Sample size 50x200 mm

Publications, reports, presentations...

- M. Jaskari, A. Järvenpää, L. P. Karjalainen, The effect of microstructure on formability of ferritic stainless steels, will be submitted to ESAFORM2020.

References of Section 2.2

1. D. Muljono, M. Ferry, D.P. Dunne, Influence of heating rate on anisothermal recrystallization in low and ultra-low carbon steels, *Mater. Sci. Eng. A.* 303 (2001) 90–99 doi:10.1016/S0921-5093(00)01882-7
2. V. Massardier, a. Ngansop, D. Fabregue, S. Cazottes, J. Merlin, Ultra-Rapid Intercritical Annealing to Improve Deep Drawability of Low-Carbon, Al-Killed Steels, *Metall. Mater. Trans. A.* 43 (2012) 2225–2236. doi:10.1007/s11661-012-1096-6
3. W.B.R. Moore, I. Salvatori, Rapid Annealing of Cold Rolled Stainless Steels, 40 (2000) 79–83
4. Y. Yazawa, Y. Ozaki, Y. Kato, O. Furukimi, Development of ferritic stainless steel sheets with excellent deep drawability by {1 1 1} recrystallization texture control, *JSAE Rev.* 24 (2003) 483–488. doi:10.1016/S0389-4304(03)00082-1
5. D. Raabe, K. Lücke, Rolling and Annealing Textures of BCC Metals, *Mater. Sci. Forum.* 157–162 (1994) 597–610. doi:10.4028/www.scientific.net/MSF.157-162.597
6. Y. Yazawa, M. Muraki, Y. Kato, O. Furukimi, Effect of Chromium Content on Relationship Between r -value and {111} Recrystallization Texture in Ferritic Steel, 43 (2003) 1647–1651
7. H. Liu, Z. Liu, G. Wang, Texture Development and Formability of Strip Cast 17 % Cr Ferritic Stainless Steel, *ISIJ Int.* 49 (2009) 890–896 doi:10.2355/isijinternational.49.890
8. C.W. Sinclair, F. Robaut, L. Maniguet, J.-D. Mithieux, J.-H. Schmitt, Y. Brechet, Recrystallization and Texture in a Ferritic Stainless Steel: an EBSD Study, *Adv. Eng. Mater.* 5 (2003) 570–574 doi:10.1002/adem.200300377

2.3 Austenitic stainless steels and grain refinement

Austenitic stainless steels are the most commonly used group of stainless steels. They possess excellent corrosion resistance, work hardening capability and formability, but relatively low yield strength in annealed condition. The research in the NorFaST-HT project focused on reversion of 3xx series (Cr-Ni) austenitic stainless steels. 3xx series steels have higher content of nickel and also better corrosion resistance, but they are mechanically weaker due to lower nitrogen content than the Cr-Mn steels in 2XX series. [1]. Excellent mechanical properties have been typically utilized to improve the strength by cold deformation (temper rolling) [2]. A disadvantage of this strengthening is the formation of anisotropy in mechanical properties [3] that limits the design possibilities e.g. in EUROCODE3 based structures [4]. So called reversion [5] treatment was studied in



NorFaST-HT project to produce ultra-high-strength austenitic steel without anisotropy by utilizing the reversion treatment to reduce the grain size down to micron–submicron size. Even though the reversion phenomenon is well-known and studied since 1990's, there are no commercial solutions for production of such steels.

The research in NorFaST-HT was focused on industrial aspects to determine the suitability of reversion for bulk steel manufacturing, but also for steel fabrication. It was shown in an earlier study [6] that the laser source can be employed to reverse cold-rolled AISI 301LN steel locally to produce similar microstructure and properties as observed in laboratory testing. Fundamental research using a Gleeble simulator was focused on austenite stability under tensile and cyclic loading. The main observation was the effect of low-temperature reversion ($T < 900\text{ °C}$) on precipitation and the stability of austenite in subsequent deformation. It was shown that the CrN precipitation occurs in the 301LN steel at reversion annealing temperatures of $\sim 700\text{--}850\text{ °C}$. The precipitation binds the austenite stabilizing nitrogen from the matrix decreasing the austenite stability. The industrial related research showed that the prior cold rolling reduction even as low as 32% can be used to produce structures having the yield strength over 800 MPa, instead of using the temper rolling. Further it was shown that induction heating can be also used for controlled reversion treatments to produce ultra-high-strength austenitic structures with the formability equal or better than that of temper-rolled counterparts.

Publications, reports, presentations...

- A. Järvenpää, Microstructures, mechanical stability and strength of a low-temperature reversion-treated AISI 301LN stainless steel under monotonic and dynamic loading, PhD thesis (defence 15.2.2019), University of Oulu, 2019.
- D. Ahmadkhaniha, Y. Huang, M. Jaskari, A. Järvenpää, M. Heydarzadeh Sohi, C. Zanella, L. P. Karjalainen, T. Langdon Effect of high-pressure torsion on microstructure, mechanical properties and corrosion resistance of cast pure Mg, Submitted and approved to J. Mater. Sci., 2018
- D. Ahmadkhani, Y. Huang, M. Jaskari, A. Järvenpää, M.H. Sohi, C. Zanella, L.P. Karjalainen, T.G. Langdon, Effect of high-pressure torsion on microstructure, mechanical properties and corrosion resistance of cast pure Mg, UFGNSM 2017 conference
- Donya Ahmadkhaniha, A. Järvenpää, M. Jaskari, M. Heydarzadeh Sohi, A. Zarei-Hanzaki, M. Fedel, F. Deflorian, L.P. Karjalainen, Microstructural modification of pure Mg for improving mechanical and biocorrosion properties, Journal of the mechanical behavior of biomedical materials, 2016.
- A.S. Hamada, A. Järvenpää, E.Ahmed, P. Sahu, A.I.Z. Farahat, Enhancement in grain-structure and mechanical properties of laser reversion treated metastable austenitic stainless steel, Materials and Design, Vol 94, 2016, P. 345–352.

2.3.1 Tensile strength

The coarse-grained commercial austenitic steel (Fig. 37a) is typically strengthened using cold rolling that increases both the yield and tensile strength of the structure due to austenite deformation and martensite transformation. As seen in Fig. 38a, cold rolling enhances especially the tensile properties, but the effect on compression strength is lower. Fine-grained reversed structures (Fig. 37b and c) are strengthened by efficient grain refinement or the presence of retained phases measured in tensile tests. The tension-compression anisotropy is thought to be negligible in reversed structures, although not determined yet. The study also showed that the cold rolling does not increase the strength of the reversed structures (Fig. 38b), but this is not big disadvantage, for the strength of the reversed structures is without any subsequent cold rolling at least as high as the strength of the commercial coarse-grained steel after 20% cold rolling. It was also noticed that in the reversed structure, the discontinuous yielding, long Luders strain, disappeared after 10% cold rolling.

Reversion studies were continued aiming at reaching the yield strength of 1000 MPa. Some of the results shown here are made in cooperation with the TERA-project (Uni. Oulu) after the NorFaST-HT -project was finished. Two different routes were designed and tested (Fig. 39) to reach the desired strength level: Route 1) optimization of prior cold rolling process and Route 2) repeated reversion treatment. The Route 1 is attractive from bulk manufacturing point of view. In contrary to laboratory trials, industrial cold rolling is not truly rolling at the ambient temperature because of high production rate. The rolling temperature varies in the range from 50 to 200 °C reducing martensite transformation so it is difficult to obtain almost martensitic structure cost-efficiently in bulk manufacturing. Route 1 allows the sheet to warm up, but it is necessary to reach the content of about 50% of martensite within the first passes. As seen from Fig. 39, very high strength level with good ductility is achieved using Route 1. Tensile tests were carried out in RD (weaker) tensile direction. One of the main



research questions for the future is, what is the anisotropy of structures created using Route 1 (including heavily deformed and recovered austenite grains) in comparison to cold rolled commercial counterparts ?

Alternatively, the strength can be increased by further grain refinement. The second reversion step (Route 2) was found to decrease the grain size from 0.6 to 0.4 μm , also homogenizing the grain size distribution leading to an increased strength level (Fig. 39). In contrary to Route 1, the twice repeated and completely reversed structure are not expected to exhibit any significant anisotropy in mechanical properties. Route 2 is not so promising for industrial bulk steel manufacturing, but the double treatment could be suitable for special cases. Some ideas for the future applications are presented in Section 3.3.

One of the main challenges with extremely fine-grained ferritic steels is the lack of work hardening capability. Austenitic stainless steels are relatively ductile also after grain refinement, but as seen especially by comparing the effect of strain rate in Fig. 39, strain hardening capability is strongly depended on the deformation conditions. The increase in the strain rate from 0.0005 to 0.008 1/s (EN 10002-2) decreases the work hardening capability. In practice, there is no work hardening in the strongest structures presented in Fig. 39 excluding in the "30% DA" structure containing a higher fraction of larger new austenite grains.

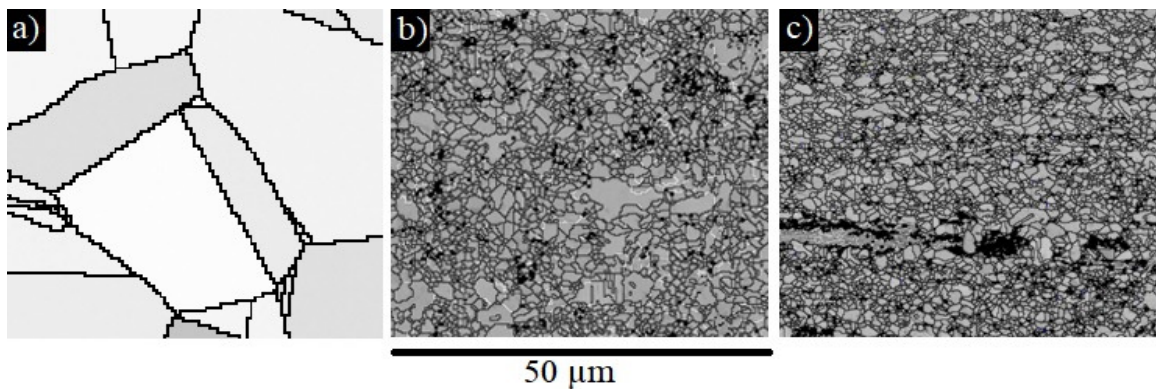


Fig. 37. Austenite grain structure for AISI 301LN in a) commercial, b) single reversed and c) twice reversed conditions.

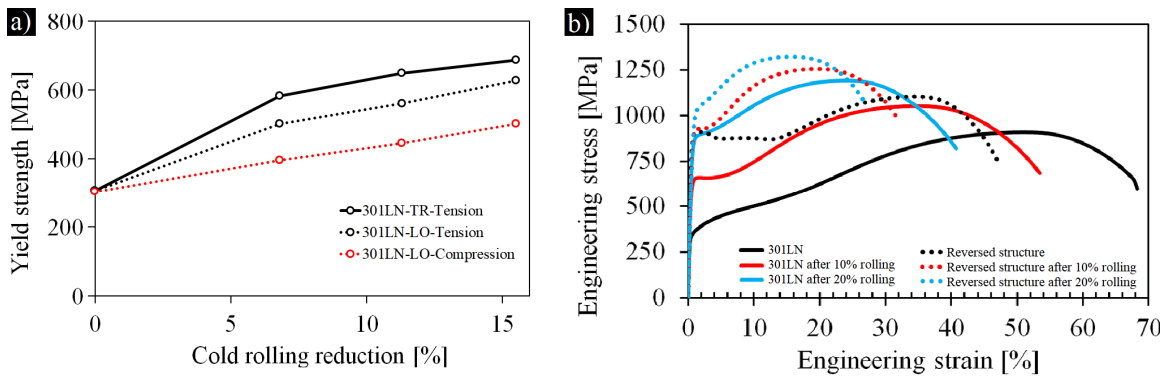


Fig. 38. Monotonic properties for cold rolled and reversed AISI 301LN showing a) anisotropy in cold rolled conditions and b) tensile test curves.

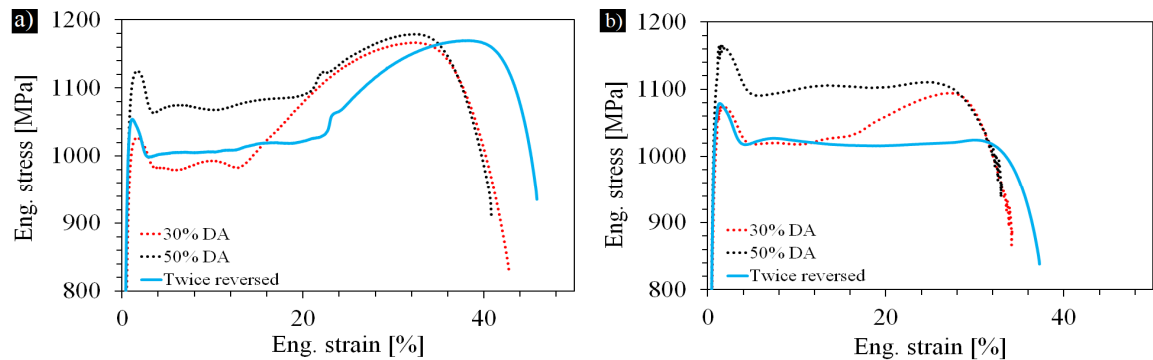




Fig. 39. Tensile curves for structures created using the newest manufacturing routes. a) low strain rate of 0.0005 1/s and b) EN 10002 strain rate. All the three structures are created using prior cold rolling reduction of 63%. The temperature was controlled to produce 50 (50% DA), 70 (30% DA) and 95% of martensite. The latter structure was cold rolled again after reversion treatment and reversion was repeated (twice). DA = retained and recovered austenite.

Publications, reports, presentations...

- A. Järvenpää, M. Jaskari, L.P. Karjalainen, Reversed Microstructures and Tensile Properties after Various Cold Rolling Reductions in AISI 301LN Steel, *Metals* 8 (2018) 109. doi:10.3390/met8020109
- A. Järvenpää, M. Jaskari, L.P. Karjalainen, Cyclic Behavior of Reversion-treated Structures after Different Cold Rolling Reductions in an AISI 301LN Stainless Steel, *Key Eng. Mater.* 786 (2018) 52-56.
- A. Järvenpää, M. Jaskari, L.P. Karjalainen, Properties of Induction Reversion-Refined Microstructures of AISI 301LN under Monotonic, Cyclic and Rolling Deformation, *Mat. Sci. Forum* 941 (2018) 601-607.
- A. Järvenpää, M. Jaskari, T. Juuti, L.P. Karjalainen, Demonstrating the effect of precipitation on mechanical stability of austenite in a reversion-treated 301LN stainless steel, *Metals* 7 (2017) 1-13.
- A. Järvenpää, M. Jaskari, J. Man, L.P. Karjalainen, Austenite stability in reversion-treated structures of a 301LN steel under tensile loading, *Mater. Charact.*, 127 (2017) 12–26.
- P. Behjati, A. Kermanpur, L.P. Karjalainen, A. Järvenpää, M. Jaskari, H. Samaei Baghbadorani, A. Najafzadeh, A. Hamada, Influence of prior cold rolling reduction on microstructure and mechanical properties of a reversion annealed high-Mn austenitic steel, *Materials Science & Engineering A*, Vol. 650, 2016, P. 119-128.
- J. Man, I. Kuběna, M. Smaga, O. Man, A. Järvenpää, A. Weidner, Z. Chlup, J. Polák, Microstructural changes during deformation of AISI 300 grade austenitic stainless steels: Impact of chemical heterogeneity, 21st European Conference on Fracture, ECF21, 20-24 June 2016, Catania, Italy, *Structural Integrity Procedia* 2, 2016, 2299-2306. <http://dx.doi.org/10.1016/j.prostr.2016.06.288>
- A. Järvenpää, M. Jaskari, M. Hietala, K. Mäntyjärvi, Local reversion of cold formed AISI 301LN, *Physics Procedia* 78, (2015) 305–311.

2.3.2 Cyclic strength

Cyclic properties and behaviour were determined for the reversed AISI 301LN structures. As seen from Fig. 40, despite the prior cold rolling reduction (32 or 56%), the fatigue strength of the reversed structures is significantly higher than in commercial 301LN. Even though the partially reversed 32CR-690-70 structure contained high fraction of retained phases, high cycle properties were not impaired due to complex microstructure. In the low-cycle region, the coarse-grained commercial 301LN showed much more efficient cyclic strain hardening. In the fine-grained reversed structures, the strength difference between the austenite and deformation-induced martensite is small so cyclic martensite formation is not effective for strain hardening. It was later shown in TERA-project that further enhancement for high-cycle fatigue strength can be achieved by repeated reversion (grain refinement). It is suggested [7] that the high-cycle strength is enhanced in reversed structures due to low strength difference between the austenite and martensite phases. The strength of the austenite is depended on the grain size so repeated reversion is one route to achieve enhanced high-cycle fatigue strength.

Both the commercial and reversed structures were subsequently cold rolled to study the effect of rolling deformation on cyclic properties and behaviour. Similarly, as observed under monotonic straining in previous Chapter, cold rolling increases the fatigue strength (Fig. 41) of the coarse-grained commercial steel much more efficiently than the one of fine-grained reversed structure. Fatigue strength of the partially reversed 56CR sheet is almost reached after 20% of cold rolling. The fatigue strength of the reversed structure is not clearly enhanced by the rolling deformation. It can be speculated that the low rolling reduction of 10% impairs and high reduction of 20% enhances slightly the fatigue strength of the reversed structure.

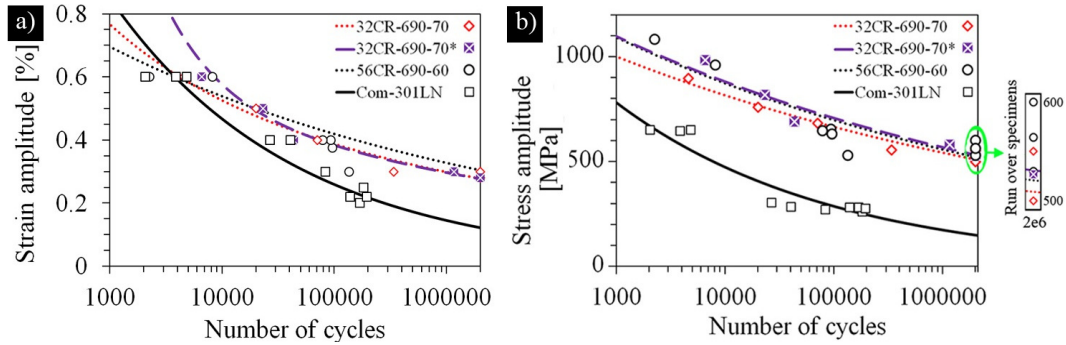


Fig. 40. Total strain amplitude vs number of cycles to failure (a) and mid-life stress amplitude vs. number of cycles to failure (b). The runover (2e6 cycles cut-off) specimens are shown in the inserts with the different y-axis scale. Load in RD direction. Coding e.g.: 32CR, 32% prior cold rolling reduction; -690, 690°C maximum temperature; -70, 70 seconds until self-cooled to 600 °C. [Antti Järvenpää, PhD thesis 2019]

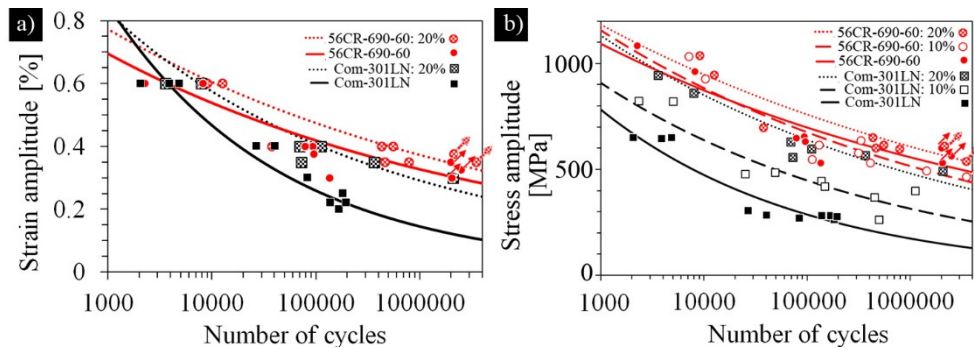


Fig. 41. Total strain amplitude vs number of cycles to failure (a) and mid-life stress amplitude vs. number of cycles to failure (b). The runover (2e6 cycles cut-off) specimens are shown in the inserts with the different y-axis scale. Load in RD direction. Coding e.g.: 56CR, 56% prior cold rolling reduction; -690, 690°C maximum temperature; -60, 60 seconds until self-cooled to 600 °C; :20%, 20% cold rolling. [Antti Järvenpää, PhD thesis 2019]

Publications, reports, presentations...

- J. Man, A. Järvenpää, M. Jaskari, I. Kuběna, S. Fintová, A. Chlupová, L.P. Karjalainen, J. Polák, Cyclic deformation behaviour and stability of grain-refined 301LN austenitic stainless structure, January 2018, MATEC Web of Conferences 165:06005 DOI: 10.1051/mateconf/201816506005
- J. Man, A. Chlupová, I. Kuběna, T. Kruml, O. Man, A. Järvenpää, L.P. Karjalainen, J. Polák, LCF behaviour of 301LN steel: coarse-grained vs. UFG-bimodal structure, in: Proceedings of the LCF8 The Eighth International Conference on Low Cycle Fatigue, Dresden, Germany, 27–29 June 2017.
- A. Järvenpää, M. Jaskari, J. Man, L.P. Karjalainen, Stability of grain-refined reversed structures in a 301LN austenitic stainless steel under cyclic loading, Mater. Sci. Eng. A 703 (2017) 280–292.
- A. Järvenpää, M. Jaskari, L.P. Karjalainen, Properties of induction reversion-refined microstructures of AISI 301LN under monotonic, cyclic and rolling deformation. Mat. Sci. Forum, 941 (2018) 601–607. <https://doi.org/10.4028/www.scientific.net/MSF.941.601>
- A. Järvenpää, M. Jaskari, L. P. Karjalainen, Grain size and austenite stability in fatigue of a reversion-treated 301LN type stainless steel, Extended abstract, NT2F16-conference, 2016.
- A.S.Hamada, A.Järvenpää, M.M.Z.Ahmed, M.Jaskari, B.P.Wynne, D.A.Porter, L.P.Karjalainen, The microstructural evolution of friction stir welded AA6082-T6 aluminum alloy during cyclic deformation, Materials Science and Engineering A 642 (2015), P. 366–376.

2.3.3 Formability

Erichsen cupping tests were carried out similarly as for ferritic stainless steels for both temper-rolled (coded TR-ASTM steel grade) and reversed structures (coded Rev). In addition to induction reversed structures, Gleeble-annealing was carried out to repeat reversion treatment once (coded 2xRev). The properties of temper-rolled and induction reversed structures are to be published in ESAFORM19 conference. Table 4 shows some



of the properties also for the twice reversed structure (2xRev). Erichsen index (IE) in relation to yield strength (YS) and uniform elongation (UE) is shown in Fig.42. The results show that the stretch formability of the reversed structures is similar or enhanced in comparison to commercial temper-rolled counterparts. It must be noted that the sample thickness has a notable effect on IE. Higher the thickness, higher the IE value. Twice repeated structure showed promising YS-IE combination (lowest sheet thickness). This 2xRev structure had also the highest measured UE value in tensile testing, but the highest IE values were measured for the softer counterparts. The IE correlates well with the YS, but there are some difference between different structures.

The 9.9 mm IE (2xRev has YS of ~1000 MPa) is similar to one observed with 2 mm thick TR-301 having the YS of 800 MPa (IE 10.4 mm). To reach similar 1000 MPa US with single reversion treatment, high amount of deformed phases has to be retained. As an example, the Rev-301LN with 1000 MPa YS (3 mm thick) showed IE of 7.7 mm. As seen by comparing the Rev-301LN structures with YS of 682 and 776 MPa, there is no clear difference in IE even though the YS is almost 100 MPa higher. Based on the results, the grain refinement enhances the formability in relation to YS more efficiently than the temper rolling.

Some brief studies were made to study the effect of punch speed on IE index. Only the 301-TR (YS ~1100 MPa) and Rev-301LN (YS ~ 1000 MPa) structures showed strain rate sensitivity (0.0002–0.04 s⁻¹). These structures showed lower IEs at lower punch speeds.

The results can be also compared with ferritic stainless steels. In comparison (Chapter 1.2.4), the IE of austenitic stainless steels is higher even at 2–3 times higher YS levels.

Table 4. Mechanical properties of the stretch formed (Erichsen test) structures.

Code	t [mm]	AGS [μm]	DIM [%]	IE [mm]	YS [MPa]	UTS [MPa]	UE [%]	TE
TR-301	3.0	19	16	10.4	800	1330	33.0	40.3
	2.0	10	40	6.0	1103	1555	22.6	28.2
TR-301LN	3.0	11	3.1	12.8	495	1044	36.3	47.1
	2.0	20	4.0	11.3	560	1041	29.0	38.4
Rev-301LN	3.0	1.0	0	12.4	682	1045	35.8	44.7
	3.0	0.9	1-2	12.3	776	1139	32.7	43.2
	3.0	0.7	15	7.7	998	1195	14.3	35.5
2xRev-301LN	0.8	0.4	1	9.9	979	1114	38.4	45.9

t, thickness; AGS, average austenite grain size; DIM, deformation-induced martensite; IE, average Erichsen index at 0.5 and 100 mm/min punch speeds; YS, yield strength; UTS, ultimate tensile strength; UE, uniform elongation; TE, total elongation

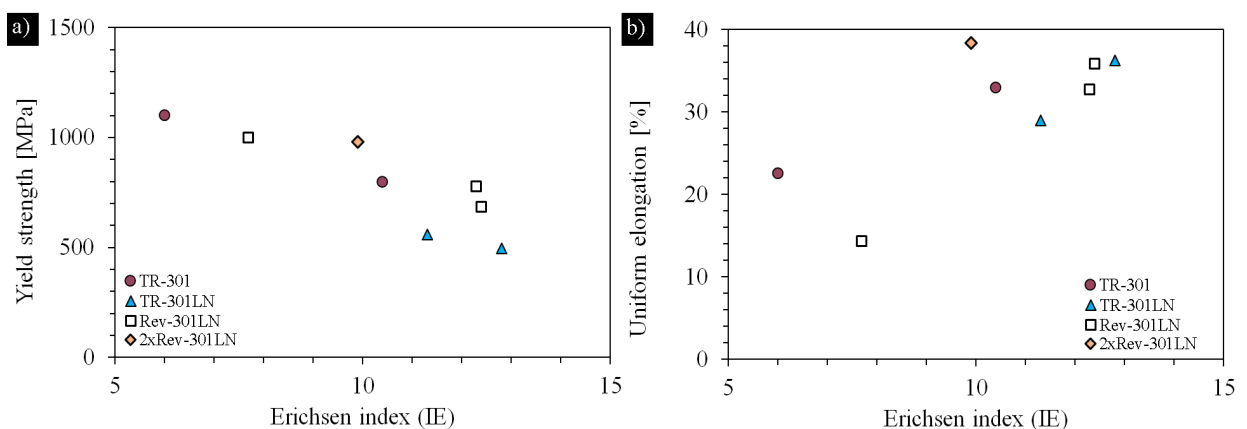


Fig. 42. Erichsen forming test results showing a) maximum cup depth in proportion to yield strength and b) example of the forming curves showing differences in fracture mechanisms.



Publications, reports, presentations...

- A. Järvenpää, M. Jaskari, M. Keskitalo, K. Mäntyjärvi & L. P. Karjalainen, Comparison of the formability of ultra-high strength austenitic reversion-treated and cold-rolled steels, submitted to ESAFORM2019 in December 2018.

2.3.4 Weldability issues

Preliminary studies were conducted to determine the effect of initial microstructure on the properties of laser-welded grain-refined AISI 301LN steel. Both the commercial temper-rolled (C1000) and reversion-treated (56% prior cold rolling reduction) sheets of 3.4 mm thickness were laser welded. The sheets were bead-on plate (without a groove) welded using a diode pumped Yb:YAG laser for microstructural analysis and testing mechanical properties of the seams. The heat input of 13.9 J/mm² was applied using constant power of 4 kW and the focal focus was 1 mm below the surface.

The hardness of the temper-rolled sheet was approximately 350 HV, whereas it is about 230 HV without the temper rolling. The hot-rolled structure consisted of austenite grains with the grain size of 20 µm. In the temper-rolled structure, 11% of the austenite was transformed to martensite and the remaining austenite grains were deformed. Two different reversion-treated structures were created: 1) completely reversed fine-grained (0.9 µm) austenitic and 2) partially reversed (~30% martensite with 10% deformed and recovered austenite) using temperatures of 790 and 660 °C and holding times (time over 600 °C) of 80 and 30 seconds, respectively. The hardness of the completely and partially reversed structures was approximately 300 and 400 HV, respectively.

As seen from Fig. 40, the hardness of the weld metal was about 250 HV and quite equal in all welded seams. Microstructures revealed that coarse-grained heat-affected zone (HAZ) was formed both in completely and partially reversed structures, the grain size being about 10 µm, whereas in the temper-rolled sheet it was 20 µm. Also, the width of the HAZ seemed to be ~20% smaller in the reversion-treated sheets. The HAZ in the reversed structures is clearly visible as narrow zone of coarse austenite grains between the weld metal and the fine-grained metal (Fig. 43). The HAZ of the temper-rolled sheet has a similar coarse grain size as the base material, but without strain-induced martensite. As seen from Fig. 43, the hardness of the weld metal was about 250 HV and quite constant in the all welded seams.

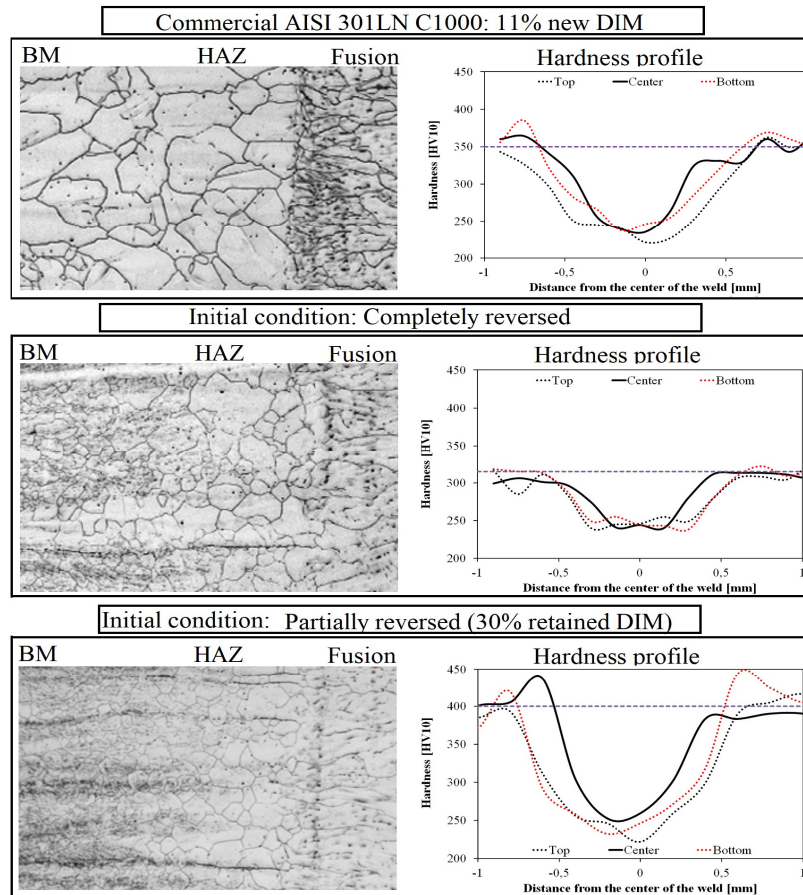


Fig. 43. The microstructure and hardness profiles for welded AISI 301LN.

The tensile strength was determined using specimens with the gauge length of 50 mm, i.e. the measured properties are average values (or the values of the weakest zone) over the whole gauge length where the weld zone is only 1–2 mm wide. All the welded tensile test specimens failed at the weld zone. As seen in Table 5, the measured YS of the joint in the partially reversed structure was distinctly highest, although it had decreased about 18% in welding, but it was still higher than the YS of the temper-rolled reference structure (C1000) before welding. The tensile elongation 14% was somewhat smaller than that of the other structures. The YS of the joint in the completely reversed structure was only slightly (-8%) affected by welding, but significant drop in the ductility was observed. Both the UE and TE were still higher in the welded condition than before welding for the C1000 or partially reversed structures. The YS of C1000 grade decreased approximately 15% by welding.

The fatigue strength (Fig. 44) was preliminary tested using few welded completely reversed and temper-rolled C1000 specimens and the results were compared with prior results for the annealed 56CR-690-60 and commercial 301LN structures (Section 1.3.2). Tests were carried out under strain-controlled loading using a relatively high strain rate (similarly as in earlier experiments). As seen from Fig. 43, the width of the laser weld, i.e. softened zone is very narrow (~1 mm). The extensometer gauge length in straining is 10 mm so we can estimate a significant strain localization in the weld zone. All the welded specimens failed along the fusion zone of the weld (low amplitudes) or at weld metal (high amplitudes).

The fatigue life of welded structures in relation to total strain amplitude (Fig. 44a) was slightly lower than the one of the annealed coarse-grained 301LN steel even though the hardness of the weld (~250 HV) was the same or slightly higher than the one of commercial annealed austenite structure (~230 HV). We can speculate that the microsegregation and/or the grain structure has some weaker sites for crack initiation and the grain size and structure is also different. Also, the weld is between harder zones which concentrates the strain to the soft narrow zone differently from strain distribution in the uniform-hardness of C1000 steel. When comparing the fatigue life to the measured stress amplitude (Fig. 44b), we notice that the welded structures are slightly stronger than the annealed 301LN structure. The monotonic yield strength of the welded structures is significantly (approximately twice) higher than one of annealed 301LN, but these high values are average values from the whole gauge length including the strong base material and soft weld. Similarly in fatigue testing, the



weld width is only about 10% of the gauge length so in the stress data, we see also the effect of the base material. It is known that the strength of a soft zone is higher if it is narrow and bordered by strong zones. Based on the results, it is clear that the fatigue strength of the welded austenitic 301LN stainless steel is low despite the original microstructure. To enhance the fatigue strength of the weld, we recommend to study the effect of reversion as a post-treatment to enhance the fatigue strength of welded austenitic stainless steel structures.

Table 5. Tensile test properties before and after welding for AISI 301LN (EN 10002-2). C1000 is commercial temper-rolled structure.

	Reversion temperature	Condition	YS	UTS	UE	TE
	°C		[MPa]	[MPa]	[%]	[%]
Completely reversed	790	BM	667	1029	39.9	54.8
		Welded	629	1012	34.2	38.7
Partially reversed	660	BM	985	1158	24.9	29.4
		Welded	810	1053	12.4	14.3
C1000	-	BM	737	1059	27.2	31.8
		Welded	629	907	26.5	27.1

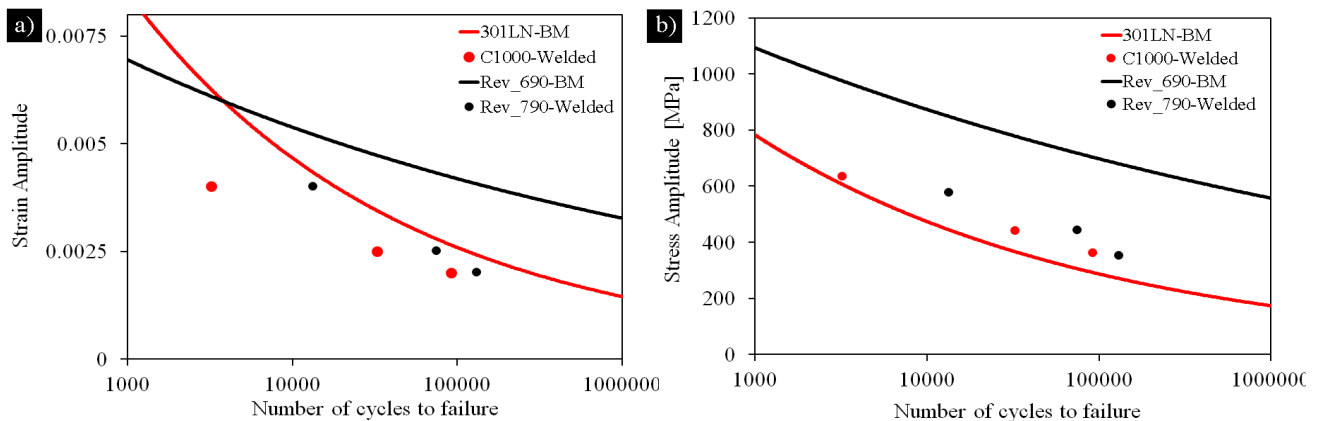


Fig.44. Fatigue life for annealed and welded AISI 301LN structures. The monotonic yield strength of the welded structures is the same (629 MPa). Data for annealed reference structures commercial 301LN and 56CR-690-60 are taken from Section 1.3.2 (Fig. 41).

Publications, reports, presentations...

- A. Järvenpää, Matias Jaskari, K. Mäntyjärvi, L. P. Karjalainen, The effect microstructure and mechanical properties of reversion treated AISI 310LN in laser welded condition, will be submitted to NoLamp2019.

2.3.5 Electromagnetic properties at high temperatures (AISI 301LN / 1.4318)

AISI 301LN (1.4318) is a highly alloyed metastable austenitic stainless steel (nominal composition shown in Table 6). Because of the metastability, both FCC or BCC phases can exist at room temperatures. The microstructure in annealed condition is the FCC structure, but cold deformation transforms the FCC structure gradually into BCC. The electric and magnetic properties are for that reason depended on the phase structure of the material when annealing below phase transformation temperatures.



Table 6. Nominal chemical composition of the alloy (in wt%).

C	Mn	Si	Cr	P	S	N	Fe
<0.03	<0.20	<1.00	16–18	<0.045	<0.03	0.07–0.2	Bal.

Measurements were carried out in two parts: 1) for the resistivity and 2) for the magnetic properties. These properties were measured on different specimens, but measured at the same time to guarantee that the properties are measured under the same conditions. The measurements were carried out after two different cold rolling conditions: 32% and 56% rolling. The measurement technique has limitations for determining the electric and magnetic properties during annealing. As seen from Fig. 45a, the same specimen is subjected to incremental increase in temperature and the properties are measured after a certain holding time. As revealed by Fig. 45b, the reversion, i.e. transformation from ferromagnetic martensite to paramagnetic austenite occurs in the temperature interval 500–700 °C. An enhanced version would be to measure the properties using similar high heating rate that is applied in practical testing and without any holding stages. Results on electric and magnetic properties and their evolution are plotted in Fig. 46. For instance, a clear difference in the magnetic permeability due to the cold rolling reductions can be seen.

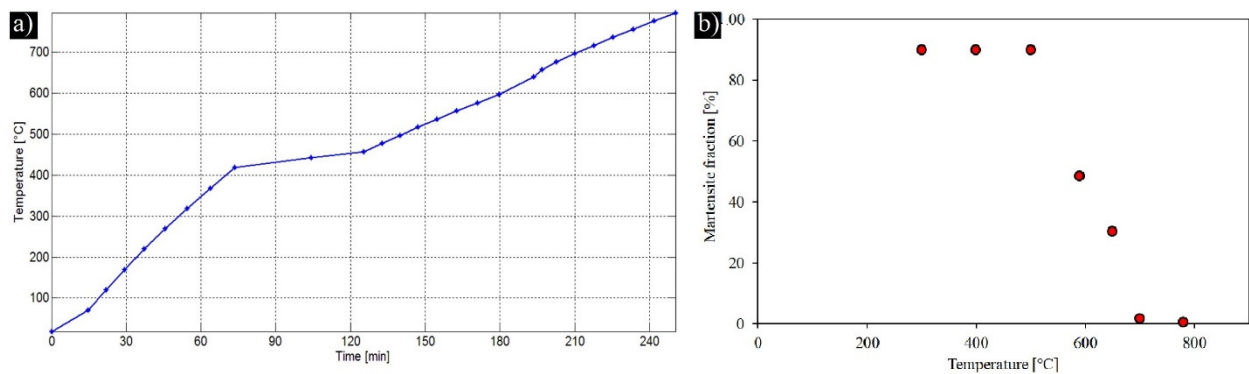


Fig. 45. a) The procedure used in Lund to measure electric and magnetic properties of cold rolled (32% and 56%) AISI 301LN showing incremental increase in temperature and b) the fraction of ferromagnetic martensite phase in 56% rolled 301LN after annealing to various temperatures using MP600 inductor in Nivala.

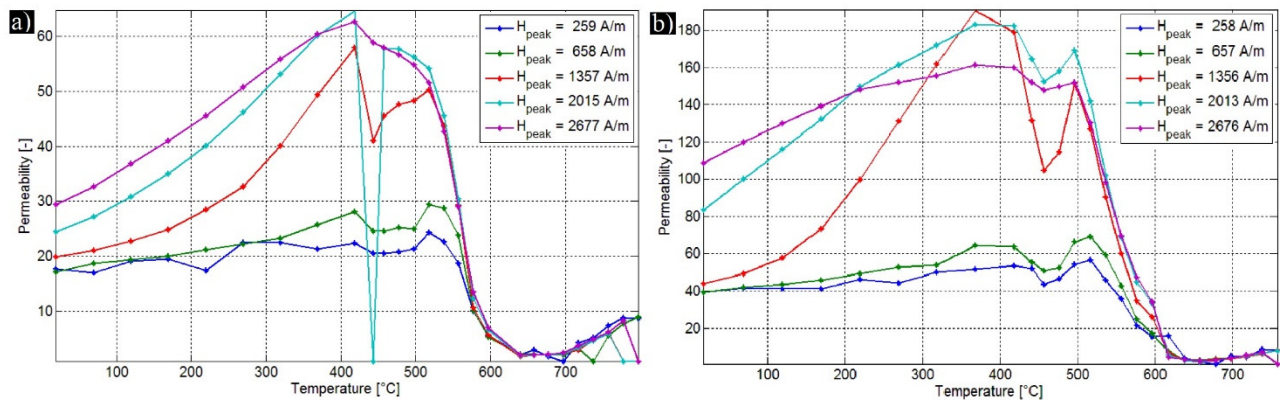


Fig. 46. Measured temperature dependency of the permeability at peak magnetic flux density for a) 32% and b) 56% cold rolled AISI 301LN.

Comparing the two conditions (32CR and 56CR) from an induction heating perspective, the difference in physical properties is not large. The small differences would give a slight advantage to the 56% condition in terms of efficiency. The 32% cold rolling would have a lower overall efficiency, especially at lower temperatures, requiring more power to keep the same heating rate as for the 56% cold rolled sheet.

The both conditions also experience a rapid degradation of the permeability at approximately 600 °C, the Curie point. At this temperature the steels transforms from ferromagnetic to paramagnetic, which usually manifests in severely decreased heating rates due the diminished efficiency. If heating beyond this point is desired with maintaining high efficiency and heating rate, special care must be taken when designing the induction coil.



Publications, reports, presentations...

- “Electric and Magnetic Data for AISI 301LN (1.4318) after 32% cold rolling”: Physical properties (Lund).
- “Electric and Magnetic Data for AISI 301LN (1.4318) after 55% cold rolling”: Physical properties (Lund).

2.4 Special processes and applications

NorFaST-HT community is not only focusing on bulk steel manufacturing processes, but also on steel fabrication. Many of the metallurgical phenomena can be utilized also locally to enhance the properties and functionality of steel products. Some of the ideas are presented here in this section.

2.4.1 Post treated welded joints

Abrasion resistant steels, i.e. hardened boron steels, are typically used in applications where welding is required for the fabrication of the components. The main problem concerning the life-time of the welded structures is the fatigue resistance of the welds. NorFaST-HT -project had a separate smaller research case to study the effect of post treatments on fatigue strength of 400 HBW wear resistant steel.

There are many factors affecting the fatigue resistance of welded structures. Firstly, hardened carbon steels exhibit very marked differences in mechanical properties across the joints: martensitic base material and the weld metal are both very hard, and between these hard zones there is typically a softened zone containing tempered martensite and ferrite-martensite dual structures. Secondly, the notch sensitivity of the material is strongly depended on the hardness. Other factors to take into account are related to the practical problems, e.g. the welding process is never ideal and is affected by many factors, e.g. human errors and/or material non-homogeneities. A major factor is, however, the residual stresses caused by welding, i.e. tensile stress with the magnitude close to the yield strength of the weld metal, which results in the fact that the fatigue limit of the steel is practically independent of the strength of the base metal. Stress relieving treatment is required to improve the situation, but it is complicated to carry out under practical conditions. One of the main research questions is if the properties of the weld metal can be restored for example by induction hardening.

As shown earlier in Section 1 (Figs. 7–9), new inductors were purchased during the NorFaST-HT project to demonstrate post treatments of pipes and beams. In addition to technological demonstration, MIG/MAG welding was employed to join the test pieces together for material characterization. Fatigue specimens were then prepared with different surface and hardening conditions. It is well known that the fatigue resistance can be enhanced by creating a compressive stress state on the surface, e.g. by surface hardening or plastic deformation by shot peening, hammering, etc. Similar effect is seen after milling (Fig. 47a). The fatigue limit of the milled and polished structures is practically the same (89 filler material joint), being equal to the base material with the production surface quality. The poorer surface quality in the milled condition is compensated by the compressive residual stresses that are absent in the electropolished condition. The untreated joints showed very low fatigue limit of less than 100 MPa. The effect of the filler material is seen in the milled condition. The 89 wire which has been observed to produce a harder weld (Fig. 47b), exhibits the fatigue limit approximately 50% higher than that of the softer counterpart. Induction hardening (MP600 unit) of the 12.51 weld increased the fatigue limit by approximately 50%. Unfortunately, there was not enough material to harden the 89 joints. The 12.51 joints were also surface hardened by laser to determine if the fatigue crack initiation (weakest link) can be transferred to other locations. The study clearly showed (insert in Fig. 47) that the crack initiation was affected by the surface hardening. Subsurface crack initiation was observed even in the low-cycle regime in surface hardened specimens. The results indicate that the local hardening or post hardening of welds can be used to reinforce the joint, but smoothening of the weld is still always necessary.

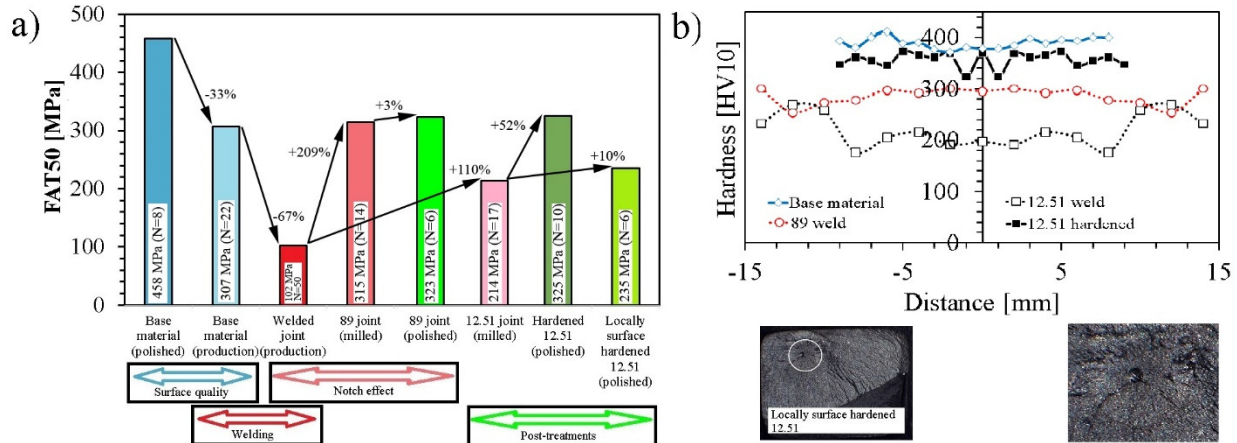


Fig. 47. Fatigue limit (FAT50) determined from S-N curves and b) hardness along the weld cross-section (top layer). The microstructural inserts show a subsurface crack initiation in surface hardened 12.51 joint after approximately 100 000 cycles. Esab OK Autorod 12.51 and Esab OK AristoRod 89 wires with 1.2 mm diameter.

Publications, reports, presentations...

- Järvenpää, M. Jaskari, M. Hietala, K. Mäntyjärvi, Local laser heat treatments of steel sheets, Physics Procedia, Vol. 78, 2015, P. 296-304.
- T. Jokelainen, A. Järvenpää, K. Saine, K. Mäntyjärvi, Iterative weight reduction process, Journal of Ship Research (2017)
- M. Kananen, K. Mäntyjärvi, M. Kesitalo, M. Hietala, A. Järvenpää, K. Holappa, K. Saine, J. Teiskonen, Laser Welded Corrugated Steel Panels in Industrial Applications, Physics Procedia 78 (2015) 202-209.
- Fatigue properties of MX400/MX500 MIG-joints: Internal mid-report

2.4.2 Surface hardened ferritic stainless steel AISI 410L (1.4003)

Ferritic stainless steel can be a low-cost alternative in many applications but the low hardness makes it susceptible to wear. In many applications, wear only occurs on localized areas of the product. Localized hardening is usually a good solution for these products in order to increase the hardness only where needed. This could be done for energy savings, but also to retain the ductility of the rest of the structure for later forming operations. Laser heating produces a high heating rate followed by rapid cooling as the bulk material acts as a heat sink.

When AISI 410L steel is subjected to the thermal cycle induced by laser heating, the ferrite transforms to austenite during annealing and transforms in turn to martensite during the fast cooling (Fig. 48). Laser surface hardening increased the hardness from ~175 HV to ~350 HV (Fig. 49) in comparison to soft initial condition. Studies showed that one-pass hardening was straight-forward and not particularly sensitive to laser parameters as long as melting is avoided. However, multiple pass hardening creates a sensitized region, which could be at risk for intergranular corrosion, where the overlapping area reaches 600–800 °C (Fig. 50). Sensitization screening was performed according to Practice W in the standard ASTM A 763-15. The sensitization occurs when chromium carbides M₂₃C₆ and nitrides Cr₂N form. These precipitations depletes the adjacent region of chromium making it prone to corrosion. A finite elemental model was also developed to study the heating cycles in order to predict where sensitization could be a risk.

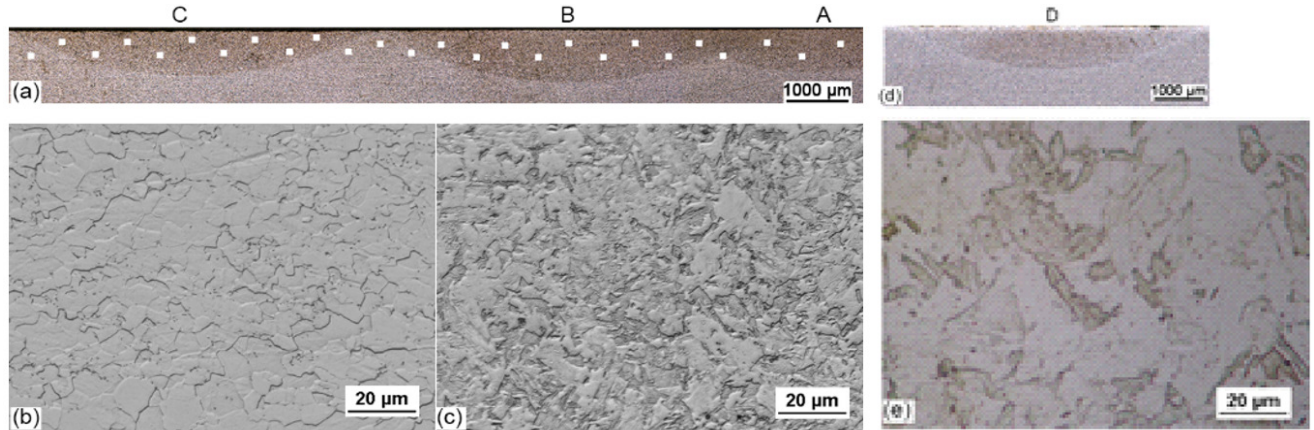


Fig. 48. a) Macrostructure of hardened tracks. b) Microstructure of base material which is completely ferritic. c) Microstructure of hardened track which is martensitic d) Single track with higher power input and e) more coarse martensite structure formed by the higher power.

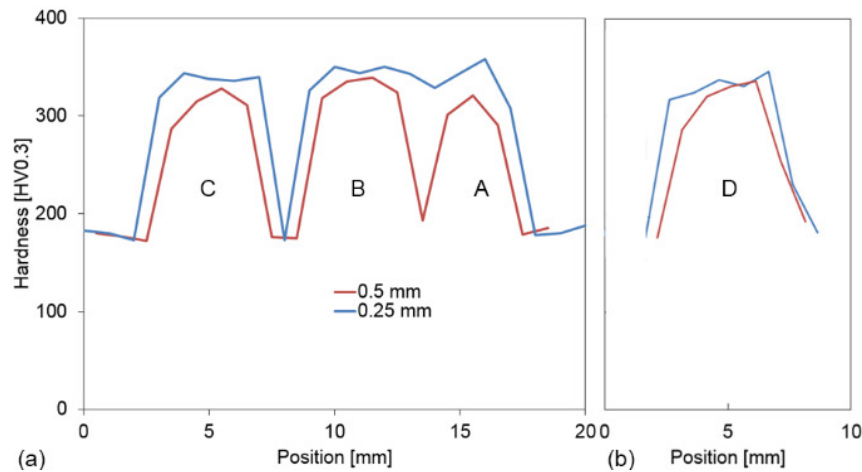


Fig. 49. a) Hardness of three adjacent tracks. b) Hardness of a single track treated with higher power.

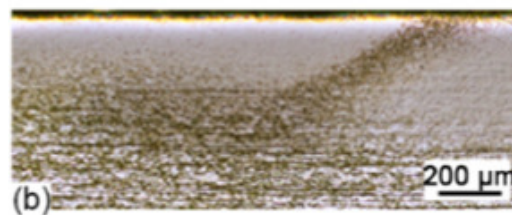


Fig. 50. Sensitised region in an overlapped track.

Publications, reports, presentations...

- J. Sundqvist, T. Manninen, H-P. Heikkinen, S. Anttila, A.F.H. Kaplan, Laser surface hardening of 11% Cr ferritic stainless steel and its sensitization behavior, Surface and Coatings Technology, Vol. 344, 2018, 673-679.

Related research:

- T. Jokelainen, A. Järvenpää, M. Keskitalo, M. Hietala, A. Mustakangas, K. Mäntyjärvi, Buckling tests for laser-welded single corrugated core, Key Eng. Mater. 786 (2018)
- M. Hietala, A. Järvenpää, M. Keskitalo, K. Mäntyjärvi, Bending Strength of Laser-welded Sandwich Steel Panels of Ultra-high Strength Steel, Key Eng. Mater. 786 (2018)
- M. Kananen, A. Järvenpää, M. Jaskari, Kari Mäntyjärvi, Mechanical Properties of a "Simple Panel Structure" Manufactured of an Ultra High Strength Stainless Steel, Key Eng. Mater. 786 (2018)



2.4.3 Drop-deposit additive manufacturing with common laser source

Since laser surface hardening of several tracks had a detrimental effect on the sensitization behavior. A novel drop-deposition technique that was recently developed at LTU was used to clad the base material. The technique employs laser remote fusion cutting on the feeding sheet, which pushes the melt on to the substrate sheet. A difference compared to hardening is that the material here reaches melting temperature and goes into the liquid phase. Laser surface hardening produced higher hardness (~350 HV) in comparison to drop-deposited specimens (~320 HV), but the main advantage of the latter is the absence of sensitization. A macro-image of three deposited tracks are shown in Fig. 51a. There is an oxide layer between the tracks due to insufficient shielding gas, but this was neglected since the sensitization behavior was in interest. Fig. 51b shows the area closest to the surface, where the ditches do not surround one whole grain while Fig. 51c shows an area in the base material, where the grains are fully surrounded. This area is by definition at risk for sensitization, but since it does not connect to the surface, this risk is avoided.

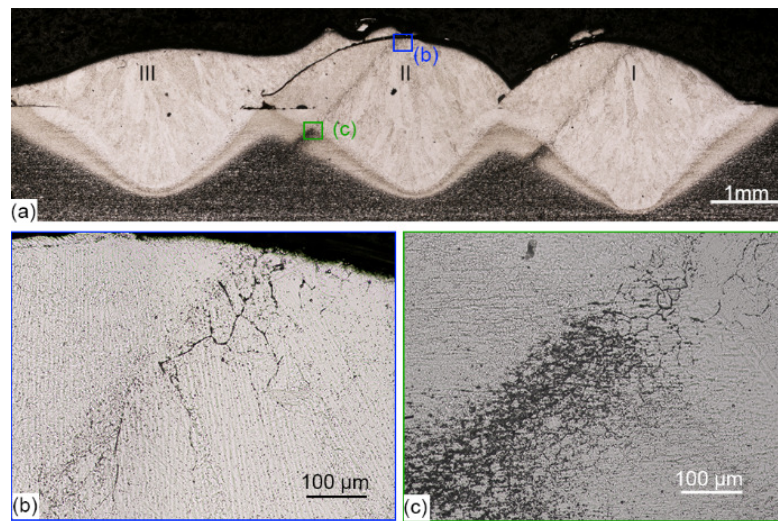


Fig. 51. (a) Macro-image of deposited tracks. (b) Area close to the surface. (c) Area where the melt transitions into base material.

Publications, reports, presentations...

- J. Sundqvist, A.F.H. Kaplan, Sensitisation behavior of drop-deposited 11% Cr ferritic stainless steel, Optics and Laser Technology, Vol. 108, 2018, 487-495.



Chapter 3 - Future induction heating and material research

The material study in the NorFaST-HT -project showed that “Fast Steel Heat Treatments” are promoting efficient grain refinement with all tested materials and also other benefits are seen in texture or carbide structures, among others. “Fast steel heat treatment” is a combination of high heating rate and short holding time, followed by controlled cooling or self-cooling. The physical laws, energy resources and pricing are setting limits for possible heating rates in industrial processing. To increase the heating rate for a certain volume of material means in practice increased power of the inductor. Similarly, the increase in volume, i.e. thickness, increases the required power linearly (2 times thickness → 2 times power). A feasible maximum heating rate in bulk steel manufacturing is ~200–400 °C/s from technological and economical points of views. For continuous processing, the time between the heating finish and start of quenching can be reduced down to few seconds. Some research laboratories have studied the effect of heating rate up to few thousand degrees per second, but the effect seems to saturate somewhere at 500 °C/s. What is the future “Fast Steel Heat Treatment” research ? What is the gain ?

- 3.1 Induction hardening and quenching & partitioning
- 3.2 Surface processing
- 3.3 Extremely “Fast Steel Heat Treatments”
- 3.4 Reversion
- 3.5 Laser processing

3.1 Induction hardening and quenching & partitioning

During the NorFaST-HT -project, some limitations in the Nivala induction line were realized and based on those findings, a new line was developed to MEFOS facilities. The MEFOS line allows a high heating rate over the whole temperature range and a high line speed allows to minimize the “holding time”, i.e. quenching begins shortly after heating. The hot rolling possibility allows also to study the effect of deformation on grain refinement. As shown in the project, induction annealing decreases the prior austenite grain size efficiently, but the strength of the martensitic structure was not strongly enhanced. The new MEFOS induction line (Section 1.2) has the readiness for the quenching & partitioning process to produce martensitic-retained austenite steels. Unfortunately, the material research during the NorFaST-HT -project was limited with the MEFOS line and the quenching & partitioning process could not be demonstrated. This work has to be performed in future projects to study the effect prior austenite refinement on properties of complex microstructures.

3.2 Surface processing

Tempering is carried out for many hardened steel grades to increase the ductility and toughness. Typically tempering is carried out in furnaces by heating the sheets for hours at a desired temperature. As shown in the literature and demonstrated in the NorFaST-HT -project, fast induction tempering produces similar or even better properties than the conventional long-lasting treatment. Induction tempering saves energy not only because of a higher efficiency, but also due to its flexibility. In contrary to furnace, inductors consume energy only when the sheets are inside the heaters.

Tempered steel grades are typically formed by bending. As shown in Fig. 52, bending stress and strain are strongly localized on the surface layers. It was shown already in another project in 2011 [Passive laser assisted bending of ultra-high strength steels] in connection with laser heating that only narrow layers can be tempered for improving the bendability of the hardened steels. In induction heating, the heat is formed inside the material surface layers. This skin-effect could be utilized in surface tempering to soften the surfaces more than the center of the sheet. Alternatively, a new approach can be selected for bulk steel tempering. It is possible to manufacture an inductor having an adjustable frequency and thereby an adjustable tempering depth. What about if the industrial tempering would be a surface tempering process where the softening depth is adjusted for each steel grade and dimensions separately ? A new project is needed to study the possibilities of surface tempering.

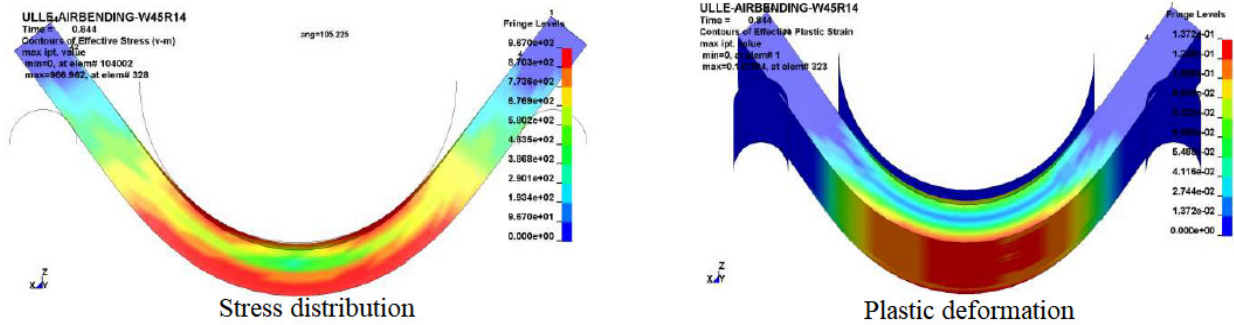


Fig. 52. Stress and strain distribution in bending process. Test material yield strength 960 MPa. [Antti Järvenpää, Master's thesis]

3.3 Extremely “Fast Steel Heat Treatments”

Lund University has developed a new power source in cooperation with the NorFaST-HT -project. The novelty of this power source is its wide frequency range from 15 kHz to 1.5 MHz, compared to that the maximum frequency of commercial equipment is less than 1 MHz. What will this kind of new equipment provide for the industry? In principle, there is a production equipment ready to either surface tempering or through tempering of bulk steel. The same unit can be adjusted for the both processes, but also for surface hardening. Is there any interest on bulk surface hardening? The new equipment can be used to introduce extremely high energy densities for sheet material. As simulated in Fig. 53, the heating rate can be over 150000 °C/s and due to extreme self-cooling, the cooling rate can be as high as 20000 °C/s. How does the material response in such an extreme heat cycle? Is there enough time for diffusional controlled processes (chemical distribution, new morphologies, etc.)? Is it possible to achieve amorphous surface with such high natural self-cooling rate?

The universities at Lund and Oulu are designing a joint project with SSAB to build a new heat treatment line utilizing this new power source. The new line will be for narrow specimens (max. width 100 mm) and for relatively short sheets (~1 m). FMT-group has already preliminary designed a proper feed system for the inductor to reach the feed speed of 3 m/s. This new line will be adopted for industrial tempering research, but also for fundamental material research aiming for entirely new observations on material behavior.

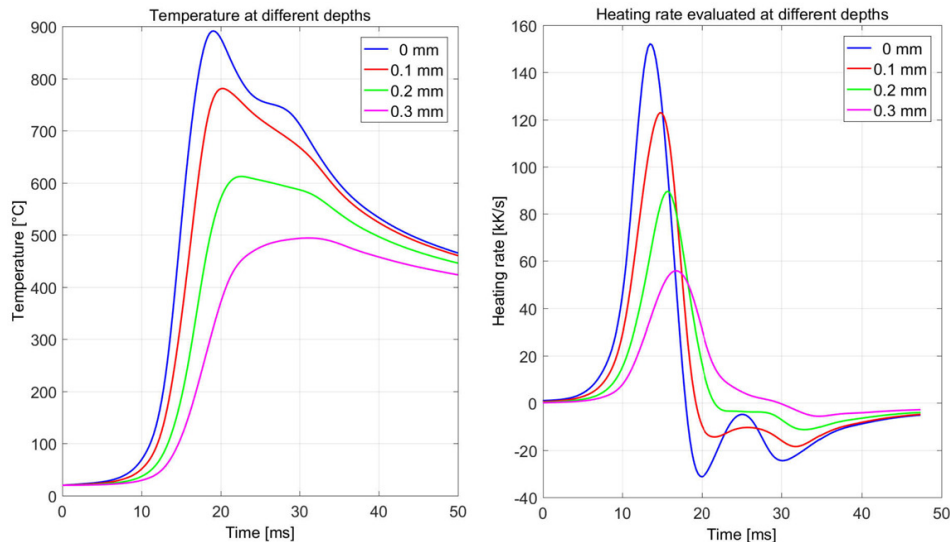


Fig. 53. Simulation results of the temperature (left) and heating/cooling rates (right) at four different distances from the surface for different time steps or positions of the strip during a transient heating operation with useful power of 30 kW and a strip speed of 1 m/s.



3.4 Reversion

Even though the reversion phenomena are extensively studied, there would still be much fundamental research needed to understand their possibilities in various applications. The future research of the community will be focused on pipe and sandwich panel applications. The NorFaST-HT -project prepared both applications. The community has an inductor for annealing the final pipes, but also to produce thin sheets for panel applications. The reversion is interesting for special processes since it can be for example repeated to enhance the properties. An experimental setup was designed to repeat the reversion multiple times to produce interesting structures especially for fundamental studies (Fig. 54). The reversion could also allow to produce seamless pipes. The idea risen in the NorFaST-HT -project is to weld a pipe using additional filler material to create a thicker weld seam along the HAZ. This thicker seam would then be cold formed by roll forming and the whole cold rolled pipe would finally be reversion-treated using induction heating.

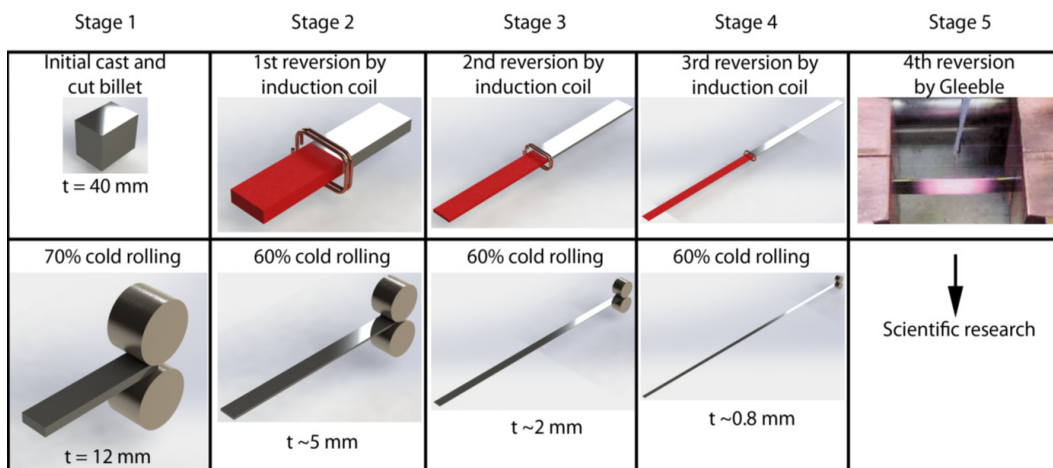


Fig. 54. Schematic illustration of experimental setup for multiple reversion treatments.

3.5 Laser processing

Based on the NorFaST-HT -project, the EU-RFCS project STIFFCRANK and the VINNOVA-project Överlag, the LTU group has decided to acquire an optical mirror system which enables shaping of the laser beam. The system has one mirror optic that can be changed in order to obtain a specially designed beam. The mirrors currently available at LTU are a 9 mm top-hat beam (a 8.8 mm Gaussian laser beam was used in NorFaSt, through defocussing, with good results) which should produce better results and a wider hardened zone than our current setup, also available at LTU are an optics that produces a line (for hardening) and two types of donut-shaped beams (intended for additive manufacturing or hardening where the temperature should be kept longer). These optics have been taken into use in September and the first results will soon be analysed. This type of optical system will enable fast switching of different beam profiles which could be interesting in industry. Changing from one beam profile to another takes less than 5 minutes, which makes it possible to do hardening of several different products with better optimised temperature cycles than a conventional laser system. In order to get the desired beam shape we will further develop our laser hardening models and expand them for more types of materials. By combining the mathematical models with the optical system, we hope to be able to tailor the laser beam and in turn the temperature cycle to optimise the laser hardening process and thereby improving the process and increasing its usefulness.

Besides hardening 'STIFFCRANK', LTU are increasing the research on processes such as surface cladding, 'Överlag' and additive manufacturing EIT-KIC RawMaterials projects, 'SPAcEMAN', 'SAMOA'. The results from NorFaST concerning microstructural properties in hardening can also be used for these processes since there are similar cooling cycles, which affect the material.